

# RSC Advances



This is an *Accepted Manuscript*, which has been through the Royal Society of Chemistry peer review process and has been accepted for publication.

*Accepted Manuscripts* are published online shortly after acceptance, before technical editing, formatting and proof reading. Using this free service, authors can make their results available to the community, in citable form, before we publish the edited article. This *Accepted Manuscript* will be replaced by the edited, formatted and paginated article as soon as this is available.

You can find more information about *Accepted Manuscripts* in the [Information for Authors](#).

Please note that technical editing may introduce minor changes to the text and/or graphics, which may alter content. The journal's standard [Terms & Conditions](#) and the [Ethical guidelines](#) still apply. In no event shall the Royal Society of Chemistry be held responsible for any errors or omissions in this *Accepted Manuscript* or any consequences arising from the use of any information it contains.

## Magnetic adsorbents on the basis of micro- and nanostructured materials.

Oxana V. Kharissova,<sup>1</sup> Rasika Dias,<sup>2</sup> Boris I. Kharisov<sup>1\*</sup>

1. Universidad Autónoma de Nuevo León, Monterrey, México.
2. The University of Texas at Arlington, USA.

\*Corresponding author. E-mail [bkhariss@hotmail.com](mailto:bkhariss@hotmail.com).

### Abstract

Micro- and nano-sized magnetic adsorbents on the basis of elemental metals, iron oxides, and ferrites, supported by inorganic (carbon, graphene, silica, zeolites) or organic (macromolecules, polysaccharides, polymers, biomolecules) compounds, are reviewed. Main attention is paid to magnetic hydrogels, xerogels, and aerogels due to their high number of environmental and biomedical applications. Role of carbohydrates and polysaccharides (starch, alginic acid, chitosan, etc.) for stabilization of magnetic nanoparticles and use the formed composites for adsorption purposes is described. Magnetic adsorbents are mainly used for heavy metals removal, separation, destruction and adsorption of oil, dyes, toxic organic compounds, several biomolecules and drugs, as well as widely in the catalytic processes. These last applications of magnetic adsorbents, in particular ferrites, are emphasized. Their main advantage for these or other possible applications is that the adsorbent or catalyst can be easily removed from reaction media after adsorption or completion of reactions via a simple magnet. Magnetic behavior studies of magnetic adsorbents are also discussed.

*Keywords:* magnetic adsorbent, nanocomposite, iron oxides, ferrites, environmental applications.

### 1. Introduction

The adsorbents formed with particles in the ranges of nano- and microsize are currently in the stage of fast development. Recently, a series of books<sup>1 2 3 4</sup> and reviews<sup>5 6</sup> have been published in this field; among them, we note an excellent comprehensive contribution dedicated to nanoadsorbents,<sup>7</sup> where adsorbent materials on the basis of metal and metal oxide nanoparticles, carbon-, silica-, and polymer-based nanomaterials, nanofibers, nanoclays, xerogels, aerogels, and destructive adsorbents are described in detail. At the same time, inside this huge research and technological area, the adsorbents possessing magnetic properties are very valuable, since their application allows a simple magnetic recovery after completion of adsorption process using magnets of distinct force. Several partial aspects of this problem are covered in recent reviews and book chapters, for example magnetically modified biological materials, containing magnetic nanoparticles as labels,<sup>8</sup> magnetic cellulose nanocomposites,<sup>9</sup> and magnetic hydrogel nanoparticles for proteins.<sup>10</sup>

In this review, we generalize most recent achievements on preparation and main applications of magnetic adsorbents, paying main attention to nano- and microsize

magnetic particles in inorganic and organic supports in the form of aerogels, hydrogels, and xerogels.

## 2. Useful definitions

**Nanocomposites.** A composite is considered as a multiphase material with significant proportion of the properties of the constituent phases, whose final product has its property improved. There is the possibility of combining various types of materials in a single composite, in order to optimize their properties according to the desired application. When one of the phases has nanometric dimension, the system is called *nanocomposite*. The interest in the preparation of magnetic nanocomposites has increased in the last years due to the properties presented by these materials, which depends on the particle size, concentration and distribution of the particles in the matrix. Nanosystems such as Fe/SiO<sub>2</sub>, Ni/SiO<sub>2</sub>, Fe<sub>3</sub>O<sub>4</sub>/SiO<sub>2</sub>, CoFe<sub>2</sub>O<sub>4</sub>/SiO<sub>2</sub>, NiFe<sub>2</sub>O<sub>4</sub>/SiO<sub>2</sub> have been intensively studied in the last years, revealing different behavior from those of bulk magnetic systems and serving as models for the study of small particles.<sup>11 12</sup>

**Xerogels and aerogels.** The drying is one of the more important steps in sol-gel process because it is possible to obtain different materials by changing the drying routes. During the drying, the solvent adsorbed inside the porous gel is removed. In this process, the gel network can collapse. There are several types of drying processes; among them the *controlled drying* and the *supercritical drying* could be mentioned.<sup>13</sup> In the controlled process, the solvent is evaporated slowly at r.t. and pressure, generating a contraction on the material, provoking the decreasing in the pore size due to the surface tension. The dry gels obtained by this process are called *xerogels* and have high porosity and specific surface area. In the supercritical drying, the wet gels are put in a reactor at high temperature and pressure, above the critical point of the system, where there is no discontinuity between the liquid and gaseous phase, avoiding capillary forces. The dry gels obtained are called *aerogels* and have higher porosity than the xerogel. As an example, carbon aerogel and xerogel were prepared by a sol-gel process that involves a polycondensation of resorcinol and formaldehyde in Na<sub>2</sub>CO<sub>3</sub> catalysis, followed by a drying step, either in supercritical conditions of CO<sub>2</sub> to aerogel obtaining or in normal conditions to xerogel obtaining, and a pyrolytic step in Ar atmosphere at 750°C for 2 h.<sup>14</sup> As an example of silica xerogels, it consists of a silica network with micro, meso and macro pores interconnected for all the bulk.<sup>15</sup> Micro pores are pores smaller than 2 nm in diameter, meso pores are the pores with diameters between 2 and 20 nm, and macro pores are larger than 20 nm. These xerogel represent monolithic porous matrices (Fig. 1), without defects after drying, changed in size after thermal treatments at high temperatures. An image of silica-titania aerogel<sup>16</sup> is shown in Fig. 2.

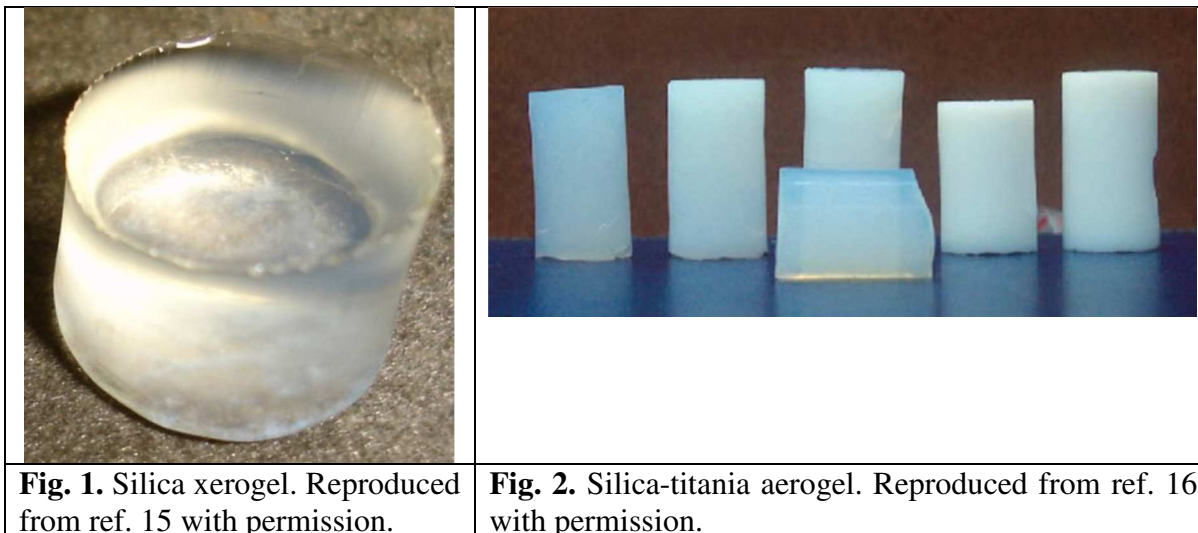


**Fig. 1.** Silica xerogel. Reproduced from ref. 15 with permission.

**Fig. 2.** Silica-titania aerogel. Reproduced from ref. 16 with permission.

**Hydrogels**<sup>17 18 19</sup> can be defined as cross-linked polymer networks which can absorb large amounts of water or biological fluids. Hydrogels themselves do not dissolve in water at a physiological temperature and pH, but swell considerably in an aqueous medium. Hydrogels are currently being considered for various biological applications such as components of drug delivery devices, microfluidic devices, biosensors, tissue implants and contact lenses. On the basis of route of their synthesis, hydrogels can be classified as:<sup>20</sup>

- Homopolymer hydrogels (made up of only one type of hydrophilic monomer);
- Copolymer hydrogels or network gels (composed of two types of monomers);
- Mutipolymer hydrogels (made up of three types of monomers or inter penetrating polymeric network).

Another mode of classification is on the basis of type of ionic charges present on polymer networks:

- Anionic hydrogels (anionic thermoassociative carboxymethylpullulan hydrogels);
- Cationic hydrogels (thermosensitive, cationic hydrogels of N-isopropylacrylamide (NIPAM) and (3-acrylamidopropyl)trimethylammonium chloride (AAPTAC));
- Neutral hydrogels (miscible blends from water-insoluble polymers like poly(2,4,4-trimethylhexamethylene terephthalamide);
- Ampholytic hydrogels (acrylamide based ampholytic hydrogels).

On the basis of physical structures hydrogels can be classified as:

- Amorphous hydrogels (chains are randomly arranged);
- Semi crystalline hydrogels (dense regions of ordered macromolecular arrangement);
- Hydrogen bonded or complexation structures (the three dimensional network formed due to hydrogen bond).

**Ferrogels.** Composed of a soft polymer matrix and magnetic filler particles, *ferrogels* are a smart materials responsive to magnetic fields. Due to the viscoelasticity of the matrix, the behaviors of ferrogel are usually rate-dependent. One of their synthesis methods is by introducing monodomain, magnetite particles of colloidal size into chemically crosslinked

poly(vinyl alcohol) hydrogels.<sup>21</sup> The ability to absorb aqueous solution without losing their shape and mechanical strength depends on the properties of the polymer, nature and the density of the network and accordingly they can absorb and retain various amount of water. Chains are connected by electrostatic force of hydrogen bond, hydrophobic interaction and such gels are not permanent. They can be converted into polymer by heating.<sup>22</sup>

**Ferrofluids** or so-called magnetic liquids are suspensions of colloid magnetic particles stabilized by surfactants in liquid media. The magnetic phase in *ferrofluids* can be represented by magnetite, ferrites (group of nonmetallic, ceramic like, usually ferromagnetic compounds of ferric oxide with other oxides) and  $\text{Fe}_x\text{C}_y$  particles resulting from the thermal decomposition of  $\text{Fe}(\text{CO})_5$ .

**Iron oxides and ferrites.** The presence of the magnetic nanoparticles (such as iron oxides or  $\text{CoFe}_2\text{O}_4$ ) inside of the inert porous matrices of xerogels and aerogels reinforce their structure, avoiding large changes in specific surface area, porosity and in the microstructure of the matrix after preparation temperature, which varied between 300 and 900°C. These characteristics influence the properties of the nanocomposites, such as their chemical reactivity, catalytic activity and magnetization. As it will be seen below, iron oxides and ferrites are generally used as magnetic phase in adsorbents. Iron oxides is a collective term for oxides, hydroxides and oxy-hydroxides composed of Fe(II) and/or Fe(III) cations and  $\text{O}^{2-}$  and/or  $\text{OH}^-$  anions. Sixteen pure phases of iron oxides, *i.e.*, oxides, hydroxides or oxy-hydroxides are known to date. These are  $\text{Fe}(\text{OH})_3$ ,  $\text{Fe}(\text{OH})_2$ ,  $\text{Fe}_5\text{HO}_8 \cdot 4\text{H}_2\text{O}$ ,  $\text{Fe}_3\text{O}_4$ ,  $\text{FeO}$ , five polymorphs of  $\text{FeOOH}$  and four of  $\text{Fe}_2\text{O}_3$ . *Maghemite* ( $\gamma\text{-Fe}_2\text{O}_3$ ) in itself is a material of great technological importance for its use in magnetic recording systems and in catalysis; moreover, maghemite properties are particularly enhanced when the size of the particles reaches the nanometer range. Although nanosized  $\gamma\text{-Fe}_2\text{O}_3$  transforms into  $\alpha\text{-Fe}_2\text{O}_3$  (hematite) at rather low temperatures (350°C) it can be stabilized through the incorporation of the nanoparticles into polymeric, glassy or ceramic matrices. Another important component in magnetic adsorbents is *magnetite*, the cubic spinel  $\text{Fe}_3\text{O}_4$ , which is ferrimagnetic at temperatures below 858 K. This mineral exhibits strong magnetic properties easily allowing creation of devices and processes for both upstream (adsorption) and downstream/deposition processes such as fixed bed adsorption, magnetically stabilized beds, magnetic separation, and remote deposition of dangerous materials. The review<sup>23</sup> refers to the adsorption/desorption possibility of the magnetite, both natural and synthetic, with respect to hazardous species dissolved in aqueous solutions. *Ferrites* are chemical compounds obtained as powder or ceramic body with ferrimagnetic properties formed by iron oxides as their main component,  $\text{Fe}_2\text{O}_3$  and  $\text{FeO}$ , which can be partly changed by others transition metals oxide. The ferrites can be classified according their crystalline structure: hexagonal ( $\text{MFe}_{12}\text{O}_{19}$ ), garnet ( $\text{M}_3\text{Fe}_5\text{O}_{12}$ ) and spinel ( $\text{MFe}_2\text{O}_4$ ), where M represents one or more bivalent transition metals (Mn, Fe, Co, Ni, Cu, and Zn).

### 3. Metal-based adsorbents

#### 3.1. Nano zero-valent iron (nZVI), other metals and alloys

As it will be seen below, iron oxides are generally used as a magnetic-responsible component in adsorbents. However, zero-valent iron has also been applied in a few magnetic nanocomposites for adsorbance purposes, mainly on the basis of carbon-

containing materials. Thus, the magnetic cellulose nanomaterials, containing nanoscale zerovalent iron (nZVI) and cellulose, were prepared by a reduction method.<sup>24</sup> With a saturation magnetization of  $57.2 \text{ emu g}^{-1}$ , the cellulose@nZVI composites could be easily separated from solutions in 30 s through the external magnetic field. Arsenite adsorption by this nano-adsorbent followed the pseudo-second-order kinetic model and Langmuir isotherm model, showing maximum removal of 99.27 %. It is necessary to mention that As(V), as well as Pb(II), Congo red and methylene blue, can be also effectively eliminated, even after five cycles, using supported nano zero-valent iron on barium ferrite microfibers.<sup>25</sup> These composite microfibers are fabricated from nano zero-valent iron and nano  $\text{BaFe}_{12}\text{O}_{19}$  grains. The enhanced adsorption characteristics can be attributed to the porous structure, strong surface activity and electronic hopping. Related zerovalent iron nanoparticles (10 nm) graphene composite (G-nZVI) is also known;<sup>26</sup> G-nZVI showed great potential as an efficient adsorbent for lead immobilization from water, as it exhibited stability, reducing power, a large surface area, and magnetic separation.

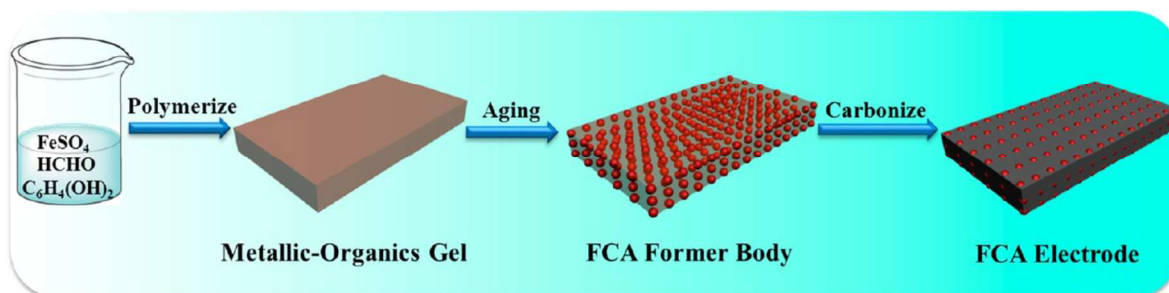
Among other carbon-containing magnetic adsorbents, mesoporous  $\text{Fe}_7\text{Co}_3$ /carbon nanocomposite was prepared *via* a cocasting method.<sup>27 28</sup> The authors noted, that by introducing  $\text{Fe}_7\text{Co}_3$  alloy nanoparticles into mesoporous carbon, the magnetic property of the nanocomposite was greatly improved compared to using a single metal Fe or Co nanoparticles. The nanocomposite was applied as magnetically separable adsorbent and exhibited excellent performance of adsorption for bulk dyes due to its high surface area ( $\leq 1429 \text{ m}^2/\text{g}$ ) and pore volume ( $\leq 1.93 \text{ cm}^3/\text{g}$ ). Related cobalt magnetic nanoparticles coated by carbon (Co/C) were prepared by catalytic chemical vapor deposition (CCVD) with ethanol.<sup>29</sup> It was shown that in the CCVD process cobalt oxide ( $\text{Co}_3\text{O}_4$ ) react with ethanol in the range  $700\text{-}900^\circ\text{C}$  producing magnetic metallic cobalt coated by different carbon materials such as graphite, and filaments. Presence of multiwalled carbon nanotubes encapsulating a cobalt metal core was confirmed. The produced Co/C nanoparticles were used as an adsorbent of organic compounds using methylene blue dye as a model molecule. In case of other metals, a green and low-cost adsorbent with both magnetic property and high adsorption capacity was prepared on the basis of nickel magnetic core with silica shell ( $\text{Ni@SiO}_2$ ).<sup>30</sup> Synthesized adsorbent exhibited higher adsorption capacity for dyes with negative charge/hydroxyl groups as compared to dyes with positive charge/without hydroxyl groups due to the hydrogen bonding interaction and electrostatic interaction between the adsorbent and dyes. The binding of these dyes with magnetic adsorbent surface mainly involves physical adsorption according to D-R model. After regeneration, the adsorbent still showed high adsorption capacity even for 4 cycles of desorption-adsorption.

#### 4. Iron oxides as magnetic adsorbents

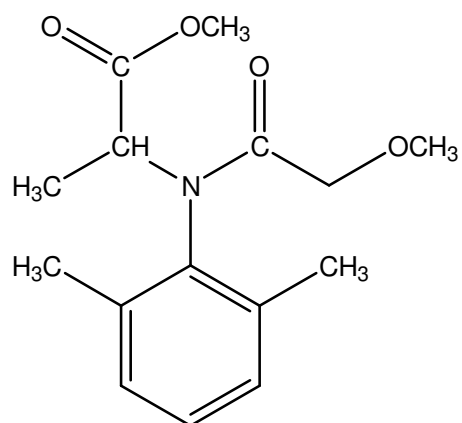
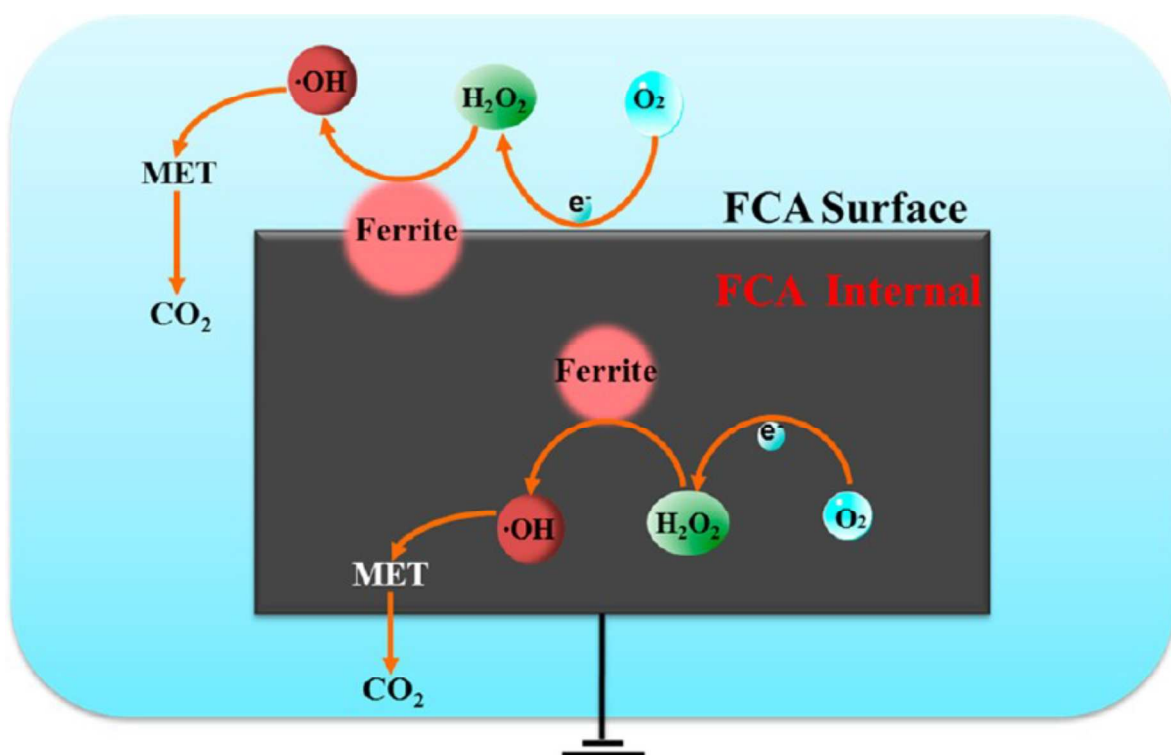
##### 4.1. Adsorbents based on the carbon matrix

A series of ferrite-carbon aerogel (FCA) monoliths with different iron/carbon ratios was synthesized<sup>31</sup> directly from metal-resin precursors accompanied by phase transformation (Fig. 3). Self-doped ferrite nanocrystals and carbon matrix were formed synchronously via moderate condensation and sol-gel processes, leading to homogeneous texture. An optimal 5% ferric content FCA was composed of coin-like carbon nano-plate with continuous porous structure, and the ferric particles with diameters of dozens of nanometers were uniformly embedded into the carbon framework. When FCA was used as an electro-Fenton

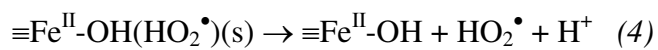
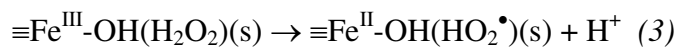
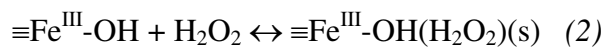
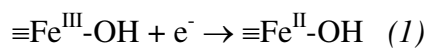
cathode (Fig. 4), metalaxyl (N-methoxyacetyl-N-(2, 6-dimethylphenyl)-DL-alaninate, **1**) degradation results demonstrated that 98% TOC elimination was realized after 4 h. It was 1.5 times higher than that of the iron oxide supported electrode. It was attributed to self-doped Fe@Fe<sub>2</sub>O<sub>3</sub> ensuring Fe(II) as the mediator, maintaining high activity *via* reversible oxidation and reduction by electron transfer among iron species with different valences (reactions 1-7). Another carbon-based magnetic aerogel photocatalysts with strong Rhodamine B (RhB) dye adsorption ability, *i.e.*, tri-functional mesoporous composite  $\gamma$ -Fe<sub>2</sub>O<sub>3</sub>/ $\alpha$ -Fe<sub>2</sub>O<sub>3</sub>/carbon aerogel (CA; its synthesis is described in<sup>32</sup>) structures, were prepared by a hydrothermal process from FeSO<sub>4</sub> as a precursor in hexamethylenetetramine (HMTA).<sup>33</sup> The as-prepared mesoporous composite  $\gamma$ -Fe<sub>2</sub>O<sub>3</sub>/ $\alpha$ -Fe<sub>2</sub>O<sub>3</sub>/CA structures have ferrimagnetic properties due to their  $\gamma$ -Fe<sub>2</sub>O<sub>3</sub> component, and they also have photocatalytic properties because of their antiferromagnetic  $\alpha$ -Fe<sub>2</sub>O<sub>3</sub> component (Fig. 5). The removal capacity of RhB dyes of the as-prepared mesoporous structures is increased from 83.5% to 91% under visible light irradiation. The mesoporous structures can also be separated by an external magnetic field to avoid further separation steps. Curiously, carbon-based aerogels can also be obtained from biomass, for example a nanocomposite of carbon aerogel and iron oxide, prepared by a facile hydrothermal treatment of watermelon.<sup>34</sup> Graphene-based magnetic adsorbents are also known; thus, macroscopic multifunctional graphene-based hydrogels with robust interconnected networks were fabricated under the synergistic effects of the reduction of graphene oxide sheets by ferrous ions and *in situ* simultaneous deposition of nanoparticles on graphene sheets.<sup>35</sup>  $\alpha$ -FeOOH nanorods and magnetic Fe<sub>3</sub>O<sub>4</sub> nanoparticles can be easily incorporated with graphene sheets to assemble macroscopic graphene monoliths just by control of pH value under mild conditions. These functional graphene-based hydrogels exhibit excellent capability for removal of pollutants and, thus, could be used as promising adsorbents for water purification. We consider graphene-based adsorbents as promising materials, under the condition of reduced cost in their massive production. For example, the present price of graphene nano platelets is \$385-525/kg and it is predicted that nanoplatelets could be produced at \$11 per kilogram.



**Fig. 3.** Illustration for fabrication of FCA electrode. Reproduced from ref. 31 with permission.

**1**

**Fig. 4.** MET degradation process in heterogeneous E-Fenton system with FCA cathode. Reproduced from ref. 31 with permission.





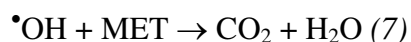
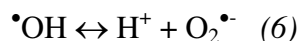
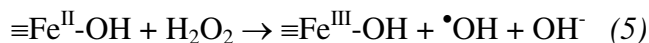


**Fig. 5.** Scheme of RhB dye removal using the as-prepared trifunctional  $\gamma$ - $\text{Fe}_2\text{O}_3$ / $\alpha$ - $\text{Fe}_2\text{O}_3$ /CA structures under visible light irradiation. The tri-functional materials can be separated with an external magnetic field. Reproduced from ref. 33 with permission.

#### 4.2. Adsorbents based on the silica and related supports

Silica is also a conventional basis for most adsorbents. Thus, the aerogel and xerogel iron oxide–silica nanocomposites were prepared by the sol–gel method.<sup>36</sup> Pure maghemite nanoparticles were obtained starting from both xerogel and aerogel samples, with particles of average size around 5 nm which tend to aggregate into the silica matrix. Variation of synthesis conditions could change resulting products. Thus, depending on the synthesis parameters, ferrihydrite or maghemite particles were obtained in similar conditions.<sup>37</sup> The material was obtained via sol–gel hydrolysis/condensation reactions of a silicon alkoxide  $\{\text{Si}(\text{OCH}_2\text{CH}_3)_4$  (TEOS) or  $\text{Si}(\text{OCH}_3)_4$  (TMOS) $\}$  with water in an alcoholic solvent, further drying by supercritical evacuation of the solvent, and growth of the magnetic phase in the silica aerogel starting from  $\text{Fe}(\text{NO}_3)_3 \cdot 9\text{H}_2\text{O}$  alone or with  $\text{FeNa}(\text{EDTA}) \cdot 2\text{H}_2\text{O}$  as precursors (Table 1). The nanoparticle phase assignments were found to be maghemite ( $\gamma$ - $\text{Fe}_2\text{O}_3$ ), magnetite ( $\text{Fe}_3\text{O}_4$ ) ferrihydrite ( $\text{Fe}_5\text{HO}_8 \cdot 4\text{H}_2\text{O}$ ). At r.t., the system was found to behave as an ensemble of non-interacting superparamagnetic particles, indicating that particle aggregation can be avoided by using a sol–gel preparation method with supercritical drying. In the temperature range from 15 to 300 K the magnetic ac susceptibility  $\chi(T)$  displayed a broad peak that shifts to higher temperatures on increasing the ac applied field frequency.

**Table 1.** Aerogel alkoxide precursor and solvents, iron salt precursor, density ( $\rho$ ), mean particle diameter ( $d_m$ ) and standard deviation ( $\sigma_d$ ) from TEM determination, activation energy ( $E$ ) for magnetic moment reversal, microscopic attempt time ( $\tau_0$ ) from the ac susceptibility, effective anisotropy constant ( $K_{\text{eff}}$ ) and magnetic phase identification. Reproduced from ref. 37 with permission.

Magnetic phase	Alkoxide and solvent	Iron salt precursor	$\rho$ (g/cm <sup>3</sup> )	$d_m$ (nm)	$\sigma_d$ (nm)	$E/k_B$ (K)	$\tau_0$ (s)	$K_{\text{eff}}$ (Jm <sup>-3</sup> )
Ferrihydrite	TEOS ethanol	Fe(NO <sub>3</sub> ) <sub>3</sub> ·9H <sub>2</sub> O	0.52	3.4	1.6			
Maghemite	TMOS methanol	Fe(NO <sub>3</sub> ) <sub>3</sub> ·9H <sub>2</sub> O	0.44	5.0	1.3	1940	10 <sup>-11</sup>	1.02·10 <sup>5</sup>
Maghemite	TMOS methanol	Fe(NO <sub>3</sub> ) <sub>3</sub> ·9H <sub>2</sub> O + FeNa(EDTA)·2H <sub>2</sub> O	0.44	4.0	1.4	1700	10 <sup>-11</sup>	1.4·10 <sup>5</sup>

Stability of these nanocomposites could be distinct in comparison with pure iron oxide nanoparticles. Thus, Fe<sub>3</sub>O<sub>4</sub>/SiO<sub>2</sub> nanocomposite aerogel powders were synthesized by a two-step process, including formation of Fe<sub>3</sub>O<sub>4</sub> nanoparticles, which were further embedded in SiO<sub>2</sub> matrix by the hydrolysis and subsequent condensation of the silicic acid.<sup>38</sup> The Fe<sub>3</sub>O<sub>4</sub>/SiO<sub>2</sub> nanocomposite were found to exhibit an enhanced thermal stability against oxidation compared with pure Fe<sub>3</sub>O<sub>4</sub>. In addition, functionalized silica-supported magnetic adsorbents were prepared and studied. Thus, the magnetic adsorbents with functional —NH<sub>2</sub> groups were synthesized by immobilization of amino-silane on the surface of the magnetic silica supports, which were prepared by co-precipitation method (Fig. 6).<sup>39</sup> These adsorbents on Fe<sub>3</sub>O<sub>4</sub> basis were applied in the separation of flavonoids {flavonoids are polyphenolic compounds and the basic structures of this matter consist of two aromatic rings (noted A and B) linked through three carbons that usually form an oxygenated heterocycle (C ring), formula **2**; they are frequently used for “greener” synthesis of metal nanoparticles using plant extracts<sup>40</sup>} from the licorice root and are shown to have selectivity to the flavonoids to some extent. The affinity selectivity of the adsorbents is based on the formation of hydrogen bonding between the —NH<sub>2</sub> groups on the magnetic adsorbents and —OH, —CO groups on the flavonoids. Another representative example of functionalization is a versatile and robust solid phase with both magnetic property and a very high adsorption capacity, presented on the basis of modification of iron oxide-silica magnetic particles with a Schiff base L (formula **3**) (Fe<sub>3</sub>O<sub>4</sub>/SiO<sub>2</sub>/L).<sup>41</sup> On its basis, an efficient and cost-effective method for the preconcentration of trace amounts of Pb(II), Cd(II) and Cu(II) in environmental and biological samples using this magnetic solid phase was offered (Fig. 7).

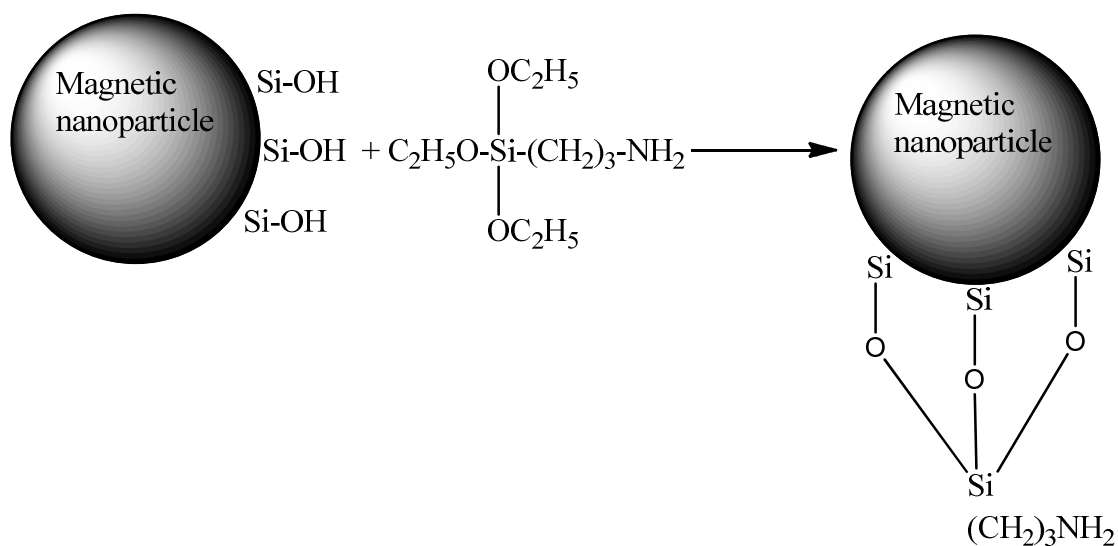
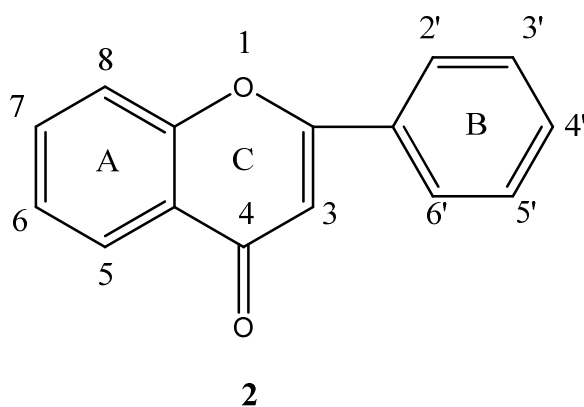
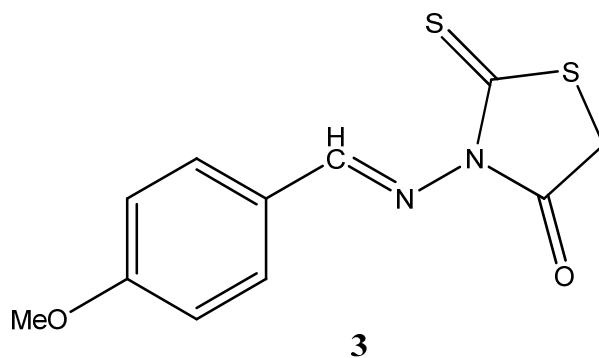


**Fig. 6.** Scheme of the coating reaction of APTS {3-aminopropyltriethoxysilane  $\text{NH}_2(\text{CH}_2)_3\text{Si}(\text{OC}_2\text{H}_5)_3$ } with magnetic silica particles.



The basic structure of flavonoids.



Structure of 3-(4-methoxybenzylideneamino)-2-thioxothiazolidin-4-one (L).

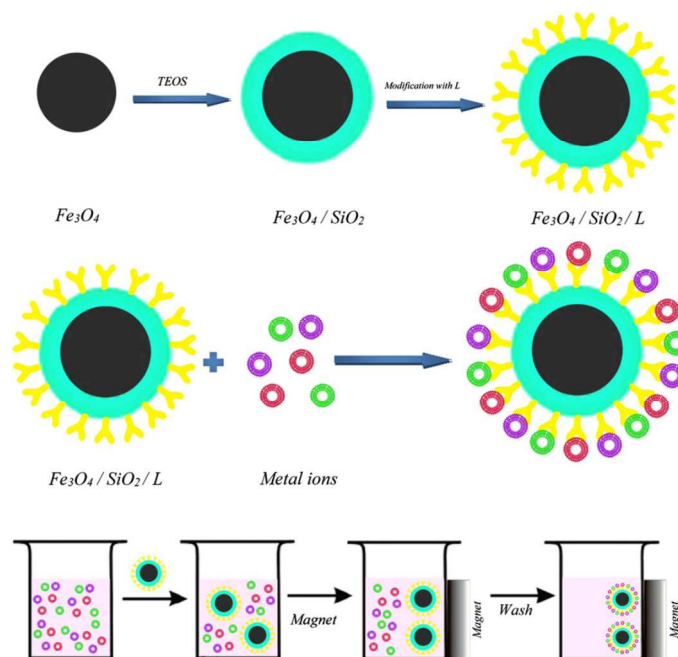


**Fig. 7.** Procedure for synthesizing Schiff base (L) modified silica-coated magnetic nanoparticles and for the proposed magnetic solid-phase extraction. Reproduced from ref. 40 with permission.

#### 4.3. Adsorbents based on the zeolites

Natural and artificial zeolites are also widespread inorganic supporting materials for micro- and nanoparticles having distinct applications.<sup>42 43 44 45 46 47</sup> Their composites-adsorbents with iron oxides can be fabricated by several routes. Thus, the zeolite was synthesized by alkaline hydrothermal treatment of coal fly ash (a major solid waste from coal-firing power stations).<sup>48 49</sup> The zeolite-iron oxide magnetic nanocomposite was prepared by mixing zeolite from coal fly ash with magnetite nanoparticles in suspension. The magnetic nanocomposite was used for the removal of U(VI) from aqueous solutions by a batch technique, as well as for adsorption of dye Reactive Orange 16. Sometimes, states of presence of nanoparticles in zeolites can be “non-conventional”. Thus, nanoparticles and nanoclusters of  $FeO(OH)/Fe_3O_4$  were incorporated by co-precipitation in the clinoptilolite channels.<sup>50</sup> The intriguing feature of this report was that the coexistence of paramagnetic and superparamagnetic Fe(III) in clinoptilolite was demonstrated. The bound of trivalent iron in clinoptilolite results in the formation iron oxide nanoclusters in microvoids, and stabilize  $AlO_4$  tetrahedral in the aluminosilicate matrix. The resulting non-framework and bound Fe(III) exhibited superparamagnetic and paramagnetic properties, respectively.

Among other zeolite-based magnetic nanocomposites, we note the adsorption features of classic zeolites (NaY, Beta, Mordenite and ZSM-5), combined with the magnetic properties of iron oxides in a composite to produce a magnetic adsorbent.<sup>51</sup> These magnetic composites can be used as adsorbents for contaminants in water and subsequently removed from the medium by a simple magnetic process. In addition, magnetic MCM-41 (from a family of silicate and aluminosilicate solids) of large surface area (ca.  $800 \text{ m}^2 \text{ g}^{-1}$ ) and high

magnetization (*ca.* 8.3 emu·g<sup>-1</sup>) was prepared at a reasonable iron oxide nanoparticles loading of 10 wt. % by a two-step synthesis process.<sup>52</sup> The 8 nm iron oxide nanoparticles (*i.e.*, 30 m<sup>2</sup>·g<sup>-1</sup>) were embedded in the MCM-41 with no observable effects on the particle morphology and pore symmetry, but a slight change (*i.e.*, <20%) in the textural properties and surface chemistry was detected. After absorption of As(V) and Cr(VI) oxyanions, this magnetic adsorbent was easily dispersed in aqueous solution and can be removed by a magnet (1550 G) at a rate of 1 cm·min<sup>-1</sup> compared to 0.004 cm·min<sup>-1</sup> by gravity.

#### 4.4. Adsorbents based on the macromolecules

Magnetic cucurbituril (MQ[n]), a functional material compound, was prepared (Fig. 8) *via* chemical co-precipitation method as a high-capacity adsorbent for humic acid (HA).<sup>53</sup> Q[n], a family of macrocyclic host molecules,<sup>54</sup> possessing its unique structure of centre hydrophobic cavity and hydrophilic portals that can form stable clathrate compounds with guest molecules through van der Waals interaction, hydrophobic interaction, electrostatic interaction, hydrogen bonding, ion–dipole or dipole–dipole interaction. Q[n] was found to be grafted on the surface of Fe<sub>3</sub>O<sub>4</sub>. MQ[n] demonstrated good adsorption capacity at pH 7 in adsorption experiments; moreover, the capacity of MQ[n] was also above 80% after being used for four times, so it may have potential industrial applications.

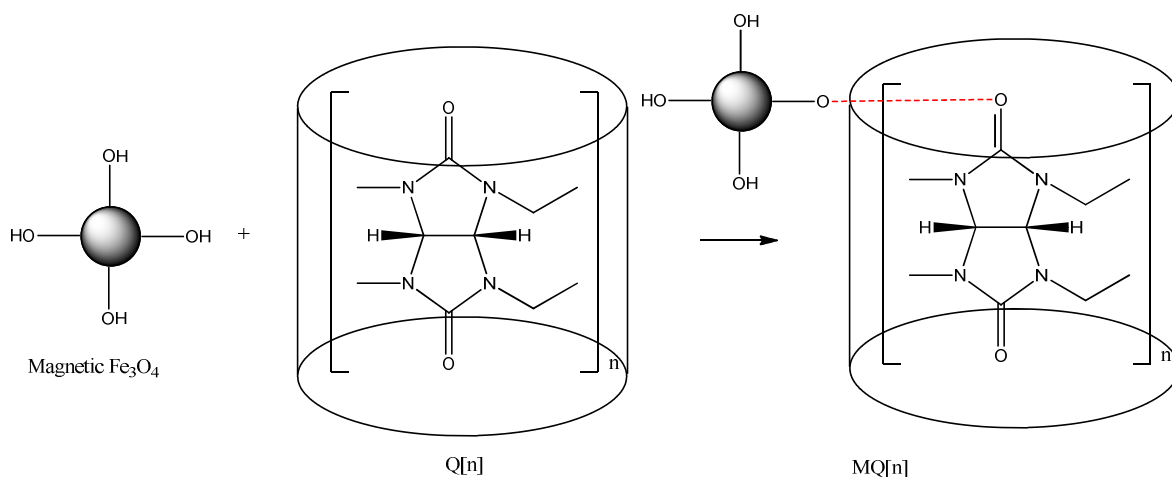


**Fig. 8.** Schematic diagrams for the formation of MQ[n].

A series of different *carbohydrates* and *polysaccharides* have been applied for stabilization of magnetic nanoparticles and use the formed composites for adsorption purposes. Thus, *starch* (**4**, Table 2) stabilized magnetic nanoparticles (SSMNPs) were prepared by reacting FeCl<sub>3</sub>·6H<sub>2</sub>O with FeCl<sub>2</sub>·4H<sub>2</sub>O in 0, 0.025, 0.5, 0.1 and 0.5% w/v of cassava waste water starch solution.<sup>55</sup> The SSMNPs were then applied in the removal of nickel ions from crude oil. The sample with the least starch concentration exhibited the strongest attraction and surface affinity for nickel complexes in crude oil with up to 93% of nickel complexes removal. Other important related objects are derivatives of *alginate acid* **5**, whose magnetic calcium alginate hydrogel beads (m-CAHBs, 3.4 mm average diameter) (Table 2) composed of γ-Fe<sub>2</sub>O<sub>3</sub> nanoparticles and calcium alginate were prepared (Fig. 9).<sup>56</sup> On their basis, the adsorption removal methodology of Cu(II) from aqueous solution by m-CAHBs

was offered. Maximum percent removal was attained under the optimum conditions with pH 2.0,  $2.0 \text{ g}\cdot\text{L}^{-1}$  adsorbent dosage for  $250 \text{ mg}\cdot\text{L}^{-1}$  initial Cu(II) ion concentration. The percent removal of Cu(II) on m-CAHBs could still be maintained at 73% level at the fifth cycle. The adsorption mechanism of Cu(II) was found to occur preferentially more by chelation than by electrostatic interaction. In addition, a spray gelation-based method was offered to synthesize a series of magnetically responsive hydrogel nanoparticles on  $\text{Fe}_2\text{O}_3$  and alginate-oligoguluronate basis for biomedical and drug delivery applications.<sup>57</sup> This method is based on the production of hydrogel nanoparticles from sprayed polymeric microdroplets obtained by an air-jet nebulization process that is immediately followed by gelation in a crosslinking fluid (Fig. 10).

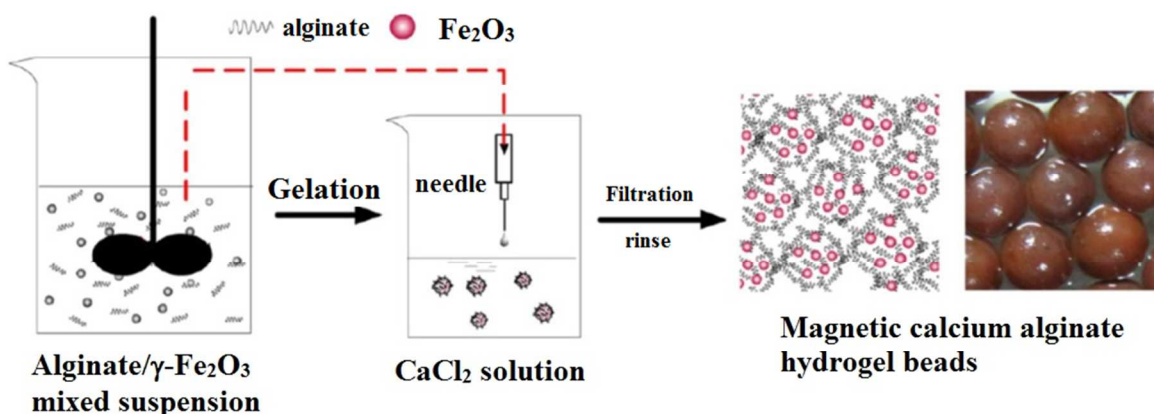


**Fig. 9.** Schematic presentation of the preparation process of m-CAHBs. Reproduced from ref. 55 with permission.

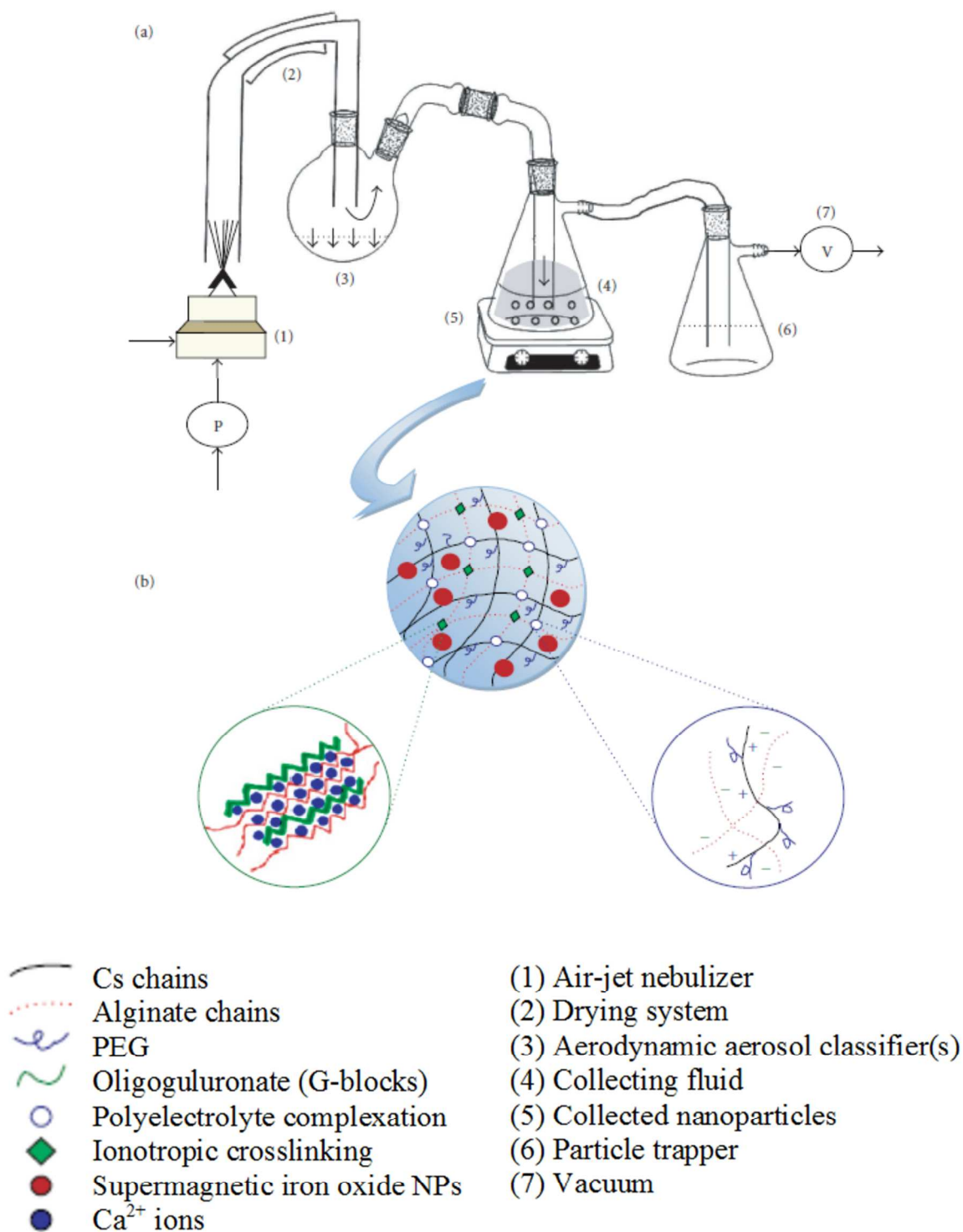


**Fig. 10.** (a) An illustration of the spray gelation-based method used in the development of the hydrogel nanoparticles. (b) Schematic illustration of the developed magnetically responsive hydrogel nanoparticles. Reproduced from ref. 56 with permission.

*Chitosan* (6, Table 2), one of favourite polysaccharides, widely applied in nanotechnology despite its low solubility, is also being frequently used. Thus, modified chitosan derivative, cross-linked with glutaraldehyde and functionalized with magnetic nanoparticles ( $\text{Fe}_3\text{O}_4$ ), was prepared for Hg(II) removal from aqueous solutions (Fig. 11).<sup>58</sup> The same  $\text{Fe}_3\text{O}_4$  nanoparticles with different size (2  $\mu\text{m}$  and 10 nm) were used for incorporation in chitosan beads (chitosan/  $\text{Fe}_3\text{O}_4$  = from 4:1 to 1:1).<sup>59</sup> The obtained magnetic beads were modified by physical cross-linking with  $\text{CuSO}_4$ , chemical crosslinking with epichlorohydrin, or were coated with a polyelectrolyte complex chitosan/poly(2-acryloylamido-2-methylpropanesulfonic acid). The magnetic beads completely sorbed a model dye - reactive red - from its aqueous solution, thus implying that such materials might be used for wastewater treatment in textile industry. In addition, with aid of oil-chitosan composite spheres, synthesized by encapsulation of sunflower seed oil in chitosan droplets (Fig. 12), hydrophilic materials (iron oxide nanoparticles) and lipophilic materials (*i.e.*, rhodamine B or epirubicin) were encapsulated.<sup>60</sup> The diameters of the prepared spheres were found to be approximately 2.5  $\mu\text{m}$  (pure chitosan spheres), 2.3  $\mu\text{m}$  (oil-chitosan composites), 1.5  $\mu\text{m}$  (iron-oxide embedded oil-chitosan composites), and 1.7  $\mu\text{m}$  (epirubicin and iron oxide encapsulated oil-chitosan composites), respectively. A lipophilic drug (epirubicin) could be loaded in the spheres with encapsulation rate measured to be 72.25%. The lipophilic fluorescent dye rhodamine B was also loadable in the spheres with red fluorescence being observed under a fluorescence microscope. Also, flat magnetic separator was used long ago to separate magnetic bioaffinity adsorbents from litre volumes of suspensions.<sup>61</sup> Both magnetic cross-linked erythrocytes and magnetic chitosan were efficiently separated; at least 95% adsorbent recovery was achieved at maximum flow rate (1680  $\text{ml}\cdot\text{min}^{-1}$ ).



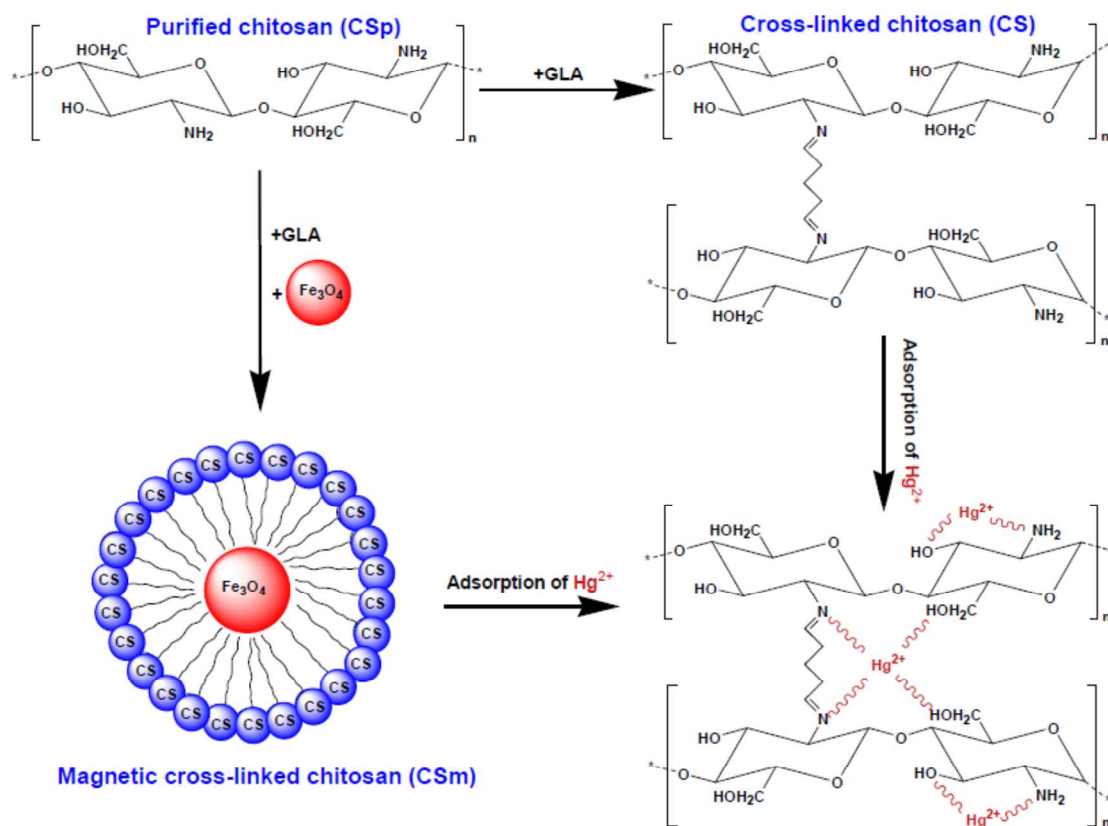


**Fig. 11.** Preparation of CS and CSm and possible interaction with Hg(II). Reproduced from ref. 57 with permission.

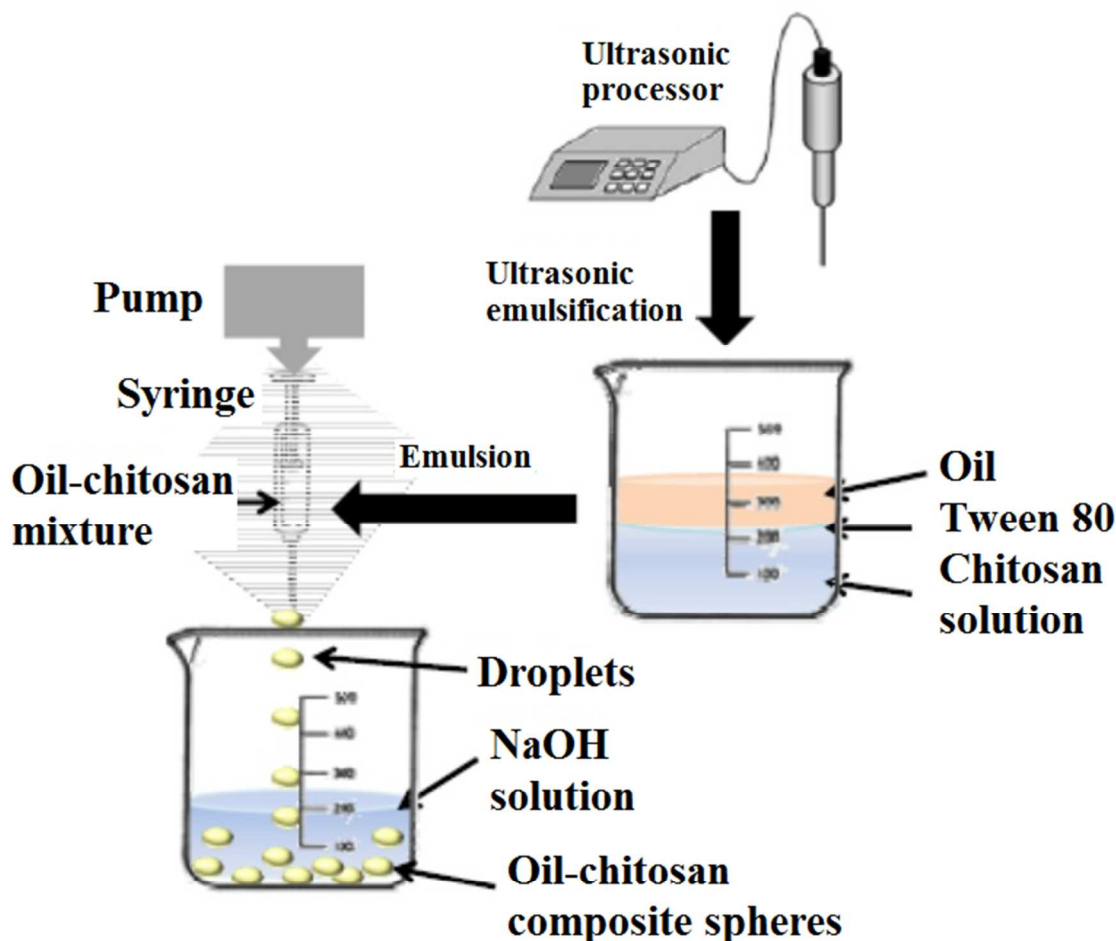


**Fig. 12.** Schematic of the preparation of oil-chitosan spheres. Reproduced from ref. 59 with permission.

#### 4.5. Adsorbents on the basis of polymers

Polymers can be considered as most common supports for magnetic nanoparticles among organic compounds and are widely used for creation of magnetic adsorbents. Thus, hydrogel nanocomposites were synthesized by incorporation of superparamagnetic  $\text{Fe}_3\text{O}_4$  particles in negative temperature sensitive poly(N-isopropylacrylamide) (7, Table 2) hydrogels.<sup>62</sup> Applying pulses of alternating magnetic field (AMF), uniform heating within the nanocomposites, leading to accelerated collapse and squeezing out large amounts of imbibed drug (release at a faster rate), took place. These smart biomaterials promise numerous potential applications in externally actuated drug delivery systems for release of drug molecules. As an example, the nanocomposite was incorporated as a valve in one of the channels of the device.<sup>63</sup> An AMF of frequency 293 kHz was then applied to the device and ON–OFF control on flow was achieved (Fig. 13). A pressure transducer was placed at the inlet of the channel and pressure measurements were done for multiple AMF ON–OFF cycles to evaluate the reproducibility of the valve. Closely related application of the same

hydrogel was also reported for the case, when  $\text{Fe}_3\text{O}_4$  nanoparticles, embedded in microrobots, can be used for propulsion and tracking in the human vascular network using an MRI platform.<sup>64</sup> The same magnetic nanoparticles can also be exploited to perform as hyperthermic actuators. When embedded in N-isopropylacrylamide thermo responsive hydrogel, vascular microrobots capable of changing their size to adapt to various diameters of blood vessels could be synthesized. This type of hydrogel is not only able to reduce size in response to temperature elevations but, as it was shown above, it can also be used to release possible therapeutic agents previously trapped within the hydrogel.

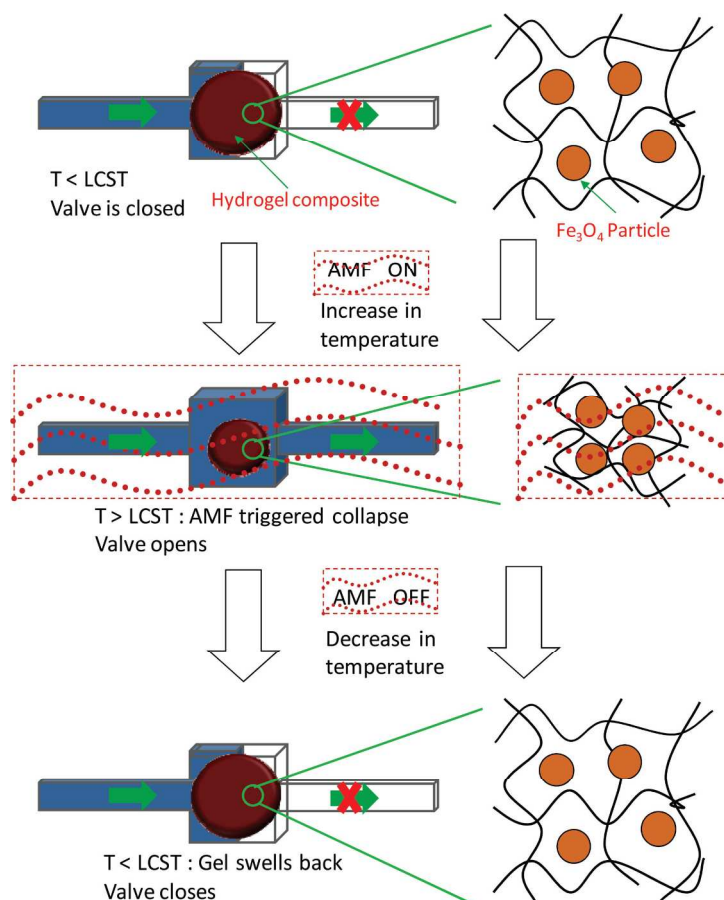


**Fig. 13.** Schematic of the concept of remote controlled hydrogel nanocomposite valves with an alternating magnetic field (AMF). Application of the AMF results in collapse of the hydrogel, leading to opening of the valve. Reproduced from ref. 62 with permission.

Magnetic field-induced heating, described above, was also explored for the purpose of developing a more effective way to recover water from swollen hydrogel draw agents.<sup>65</sup> The composite hydrogel particles were prepared by copolymerization of sodium acrylate and N-isopropylacrylamide in the presence of magnetic nanoparticles ( $\gamma\text{-Fe}_2\text{O}_3$ , size < 50 nm). It was indicated that the magnetic heating is an effective and rapid method for dewatering of hydrogels by generating the heat more uniformly throughout the draw agent particles (Fig. 14), and thus, a dense skin layer commonly formed *via* conventional heating from the outside of the particle is minimized. Significantly enhanced liquid water recovery

(53%) is achieved under magnetic heating, as opposed to only around 7% liquid water recovery obtained *via* convection heating. Also, magnetic nano-adsorbent was developed long ago using superparamagnetic  $\text{Fe}_3\text{O}_4$  nanoparticles (13.2 nm, spinel structure) as cores and polyacrylic acid (PAA, **8**, Table 2) as ionic exchange groups.<sup>66</sup> The  $\text{Fe}_3\text{O}_4$  magnetic nanoparticles were prepared by co-precipitating  $\text{Fe}^{2+}$  and  $\text{Fe}^{3+}$  ions in an ammonia solution and treating under hydrothermal conditions. PAA was covalently bound onto the magnetic nanoparticles via carbodiimide activation. The maximum weight ratio of PAA bound to the magnetic nanoparticles was revealed to be 0.12. The ionic exchange capacity of the resultant magnetic nano-adsorbents was estimated to be much higher than those of commercial ionic exchange resins. When the magnetic nano-adsorbents were used for the recovery of lysozyme, the adsorption/desorption of lysozyme was completed within 1 min due to the absence of pore-diffusion resistance.

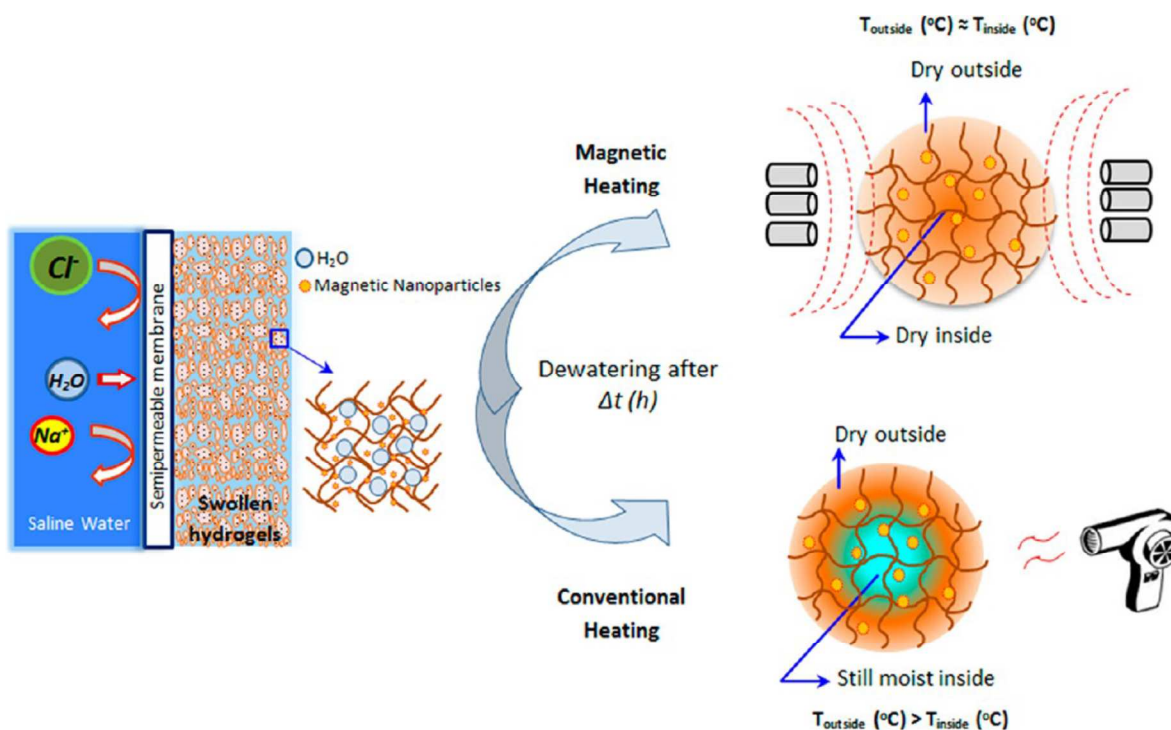


**Fig. 14.** Schematic diagram of the effect of magnetic and conventional heating on the dewatering of nanocomposite polymer hydrogels being used as draw agents in the Forward osmosis process. Reproduced from ref. 64 with permission.

Superparamagnetic hydrogel microparticles in spherical and non-spherical forms ( $\gamma\text{-Fe}_2\text{O}_3$ )<sup>67</sup> were prepared in the T-junction microfluidic channel (Figs. 15-16). The precursor (magnetic solution) consisted of poly(ethylene glycol)(700) diacrylate, (PEGDA, **9**, Table 2), deionized water, and the ferrofluid (4:4:2 in volume) with Darocur 1173 and Irgacure 819 photoinitiators. Light mineral oil with 3% ABIL EM 90 served as a continuous phase. In addition, well-defined, magnetic shell cross-linked nanoparticles (MSCKs) with hydrodynamic diameters *ca.* 70 nm were constructed through the co-assembly of amphiphilic block copolymers of PAA<sub>20</sub>-b-PS<sub>280</sub> and oleic acid-stabilized magnetic iron oxide nanoparticles using tetrahydrofuran, N,N-dimethylformamide, and water, ultimately transitioning to a fully aqueous system (Fig. 17).<sup>68</sup> These well-defined nanoparticles

showed efficient oil sorption capacity of 10-fold their initial dry weight when introduced into an aqueous environment polluted with a complex crude oil. Once loaded, the crude oil-sorbed nanoparticles were easily isolated *via* the introduction of an external magnetic field.

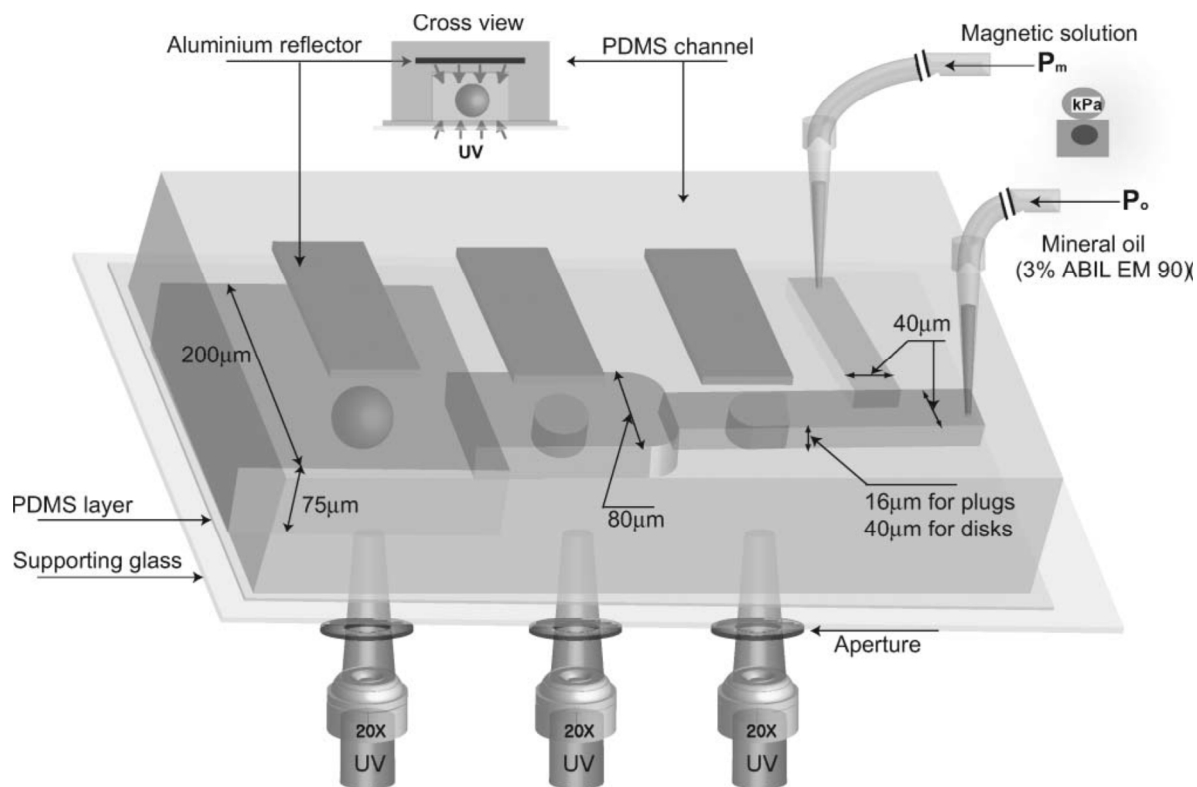


**Fig. 15.** Schematic diagram of the T-junction microfluidic channel with aluminium reflectors for spherical and non-spherical magnetic hydrogel synthesis: sphere, disk, and plug.  $P_m$  indicates the input pressure for the hydrogel precursors (dispersed phase) and  $P_o$  the input pressure for the mineral oil (continuous phase). Reproduced from ref. 66 with permission.

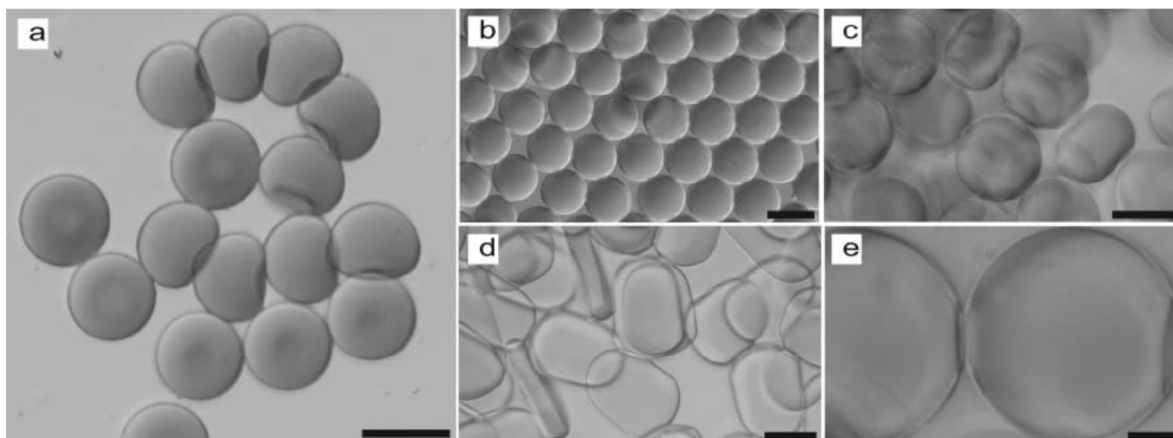


**Fig. 16.** Optical images of (a) deformed spherical magnetic microhydrogels in the absence of the aluminium UV reflector and (b)–(e) collections of magnetic microhydrogels in the presence of the aluminium UV reflector: (b) spheres, (c) disks, (d) plugs, and (e) high resolution of the disks. The scale bars are (a)–(d) 30 mm and (e) 10 mm. Reproduced from ref. 66 with permission.

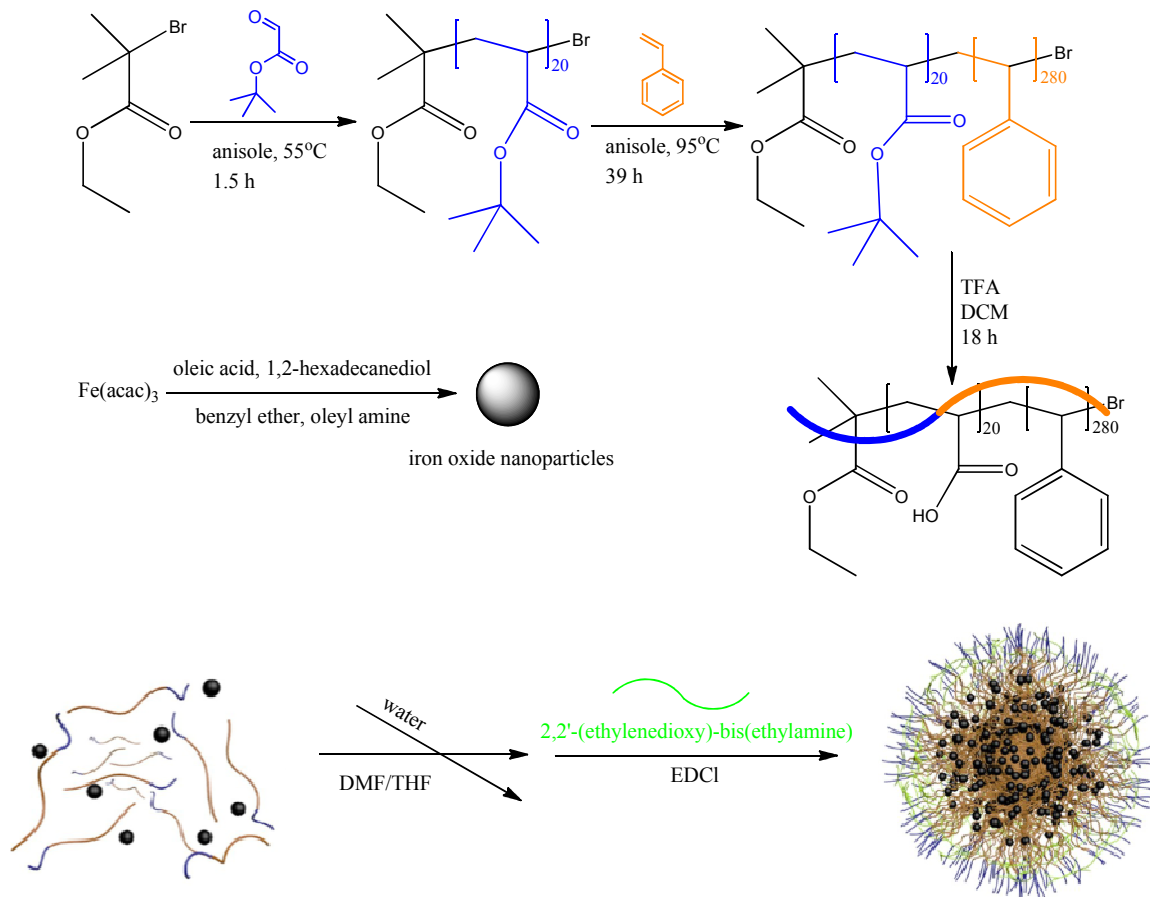


**Fig. 17.** Schematic representation of the construction of magnetic shell cross-linked (MSCK) nanoparticles. Reproduced from ref. 67 with permission.

Micro-size (average size 1  $\mu\text{m}$ , range 500 nm – 2  $\mu\text{m}$ ) magnetic polymer adsorbent (MPA) coupling with metal chelating ligands of iminodiacetic acid (IDA) and its application for the removal of Cu(II) ion was synthesized on magnetite basis.<sup>69</sup> Fe<sub>3</sub>O<sub>4</sub> nanoparticles (10 nm in size) were prepared *via* the chemical co-precipitation method and then coated with polyvinyl acetate (PVAC, **10**, Table 2) *via* the suspension polymerization with vinyl acetate (VAC), yielding magnetite-PVAC (denoted as M-PVAC). Several sequential procedures, including alcoholysis, epoxide activation, and coupling of IDA were subsequently employed to introduce functional groups on the surface of super-paramagnetite particles of M-PVAC, yielding magnetite-polyvinyl alcohol (M-PVAL), magnetite-polyvinyl propenepoxide (M-PVEP), and magnetite-polyvinyl acetate-IDA (M-PVAC-IDA), respectively. Copper ions can be adsorbed from solutions with its aid; the adsorption capacity is highest at pH value of 4.5 while decreases as the pH value decreases. Thus, the

exhausted M-PVAC-IDA after removing Cu(II) ion at moderate pH value of 4.5 can be regenerated at low pH value of 1.

#### 4.6. Adsorbents on the basis of biomolecules

A stable magnetic nanocomposite of collagen and superparamagnetic iron oxide nanoparticles (SPIONs, 10 nm) was prepared by a simple process utilizing protein wastes from leather industry.<sup>70</sup> This nanocomposite exhibited selective oil absorption and magnetic tracking ability, allowing it to be used in oil removal applications.

### 5. Ferrites as magnetic adsorbents

In addition to magnetic iron oxides, several metal ferrites have also been used as components in magnetic adsorbents, although in lesser grade in comparison with monometal iron-containing composites. As far back as in 1997, fine powders of zinc ferrite nanoparticles (ZFN)  $\text{ZnFe}_2\text{O}_4$  with an average particle size of 10 nm and inversion parameter of 0.21 were synthesized by the aerogel procedure.<sup>71</sup> Portions of the powders were calcined in air at 500 and 800°C and other portions were ball-milled for 10 h. The magnetic state of the as-produced and calcined samples is best described as disordered and highly dependent on temperature. The magnetic properties of the ball-milled sample are similar to those of ferrimagnetic  $\text{MgFe}_2\text{O}_4$  powders having comparable grain size and inversion parameters. In a related report,<sup>72</sup> monolithic zinc ferrite aerogels were produced by the epoxide addition sol-gel method (addition of propylene oxide to 2-propanol solution of either the hydrated metal nitrate salts or the hydrated metal chloride salts resulting in the formation of stable red-brown gels). All synthesized aerogels exhibited low densities and high surface areas (340  $\text{m}^2/\text{g}$ ). Annealing of the aerogel at relatively lower temperatures (below 450°C) in comparison with the method above yielded a highly crystalline porous material which was composed of nanometer sized particles (Fig. 18). In addition, zinc-ferrite nanoparticles can be non-stoichiometrical: this their property was studied as a function of the particle size.<sup>73</sup>

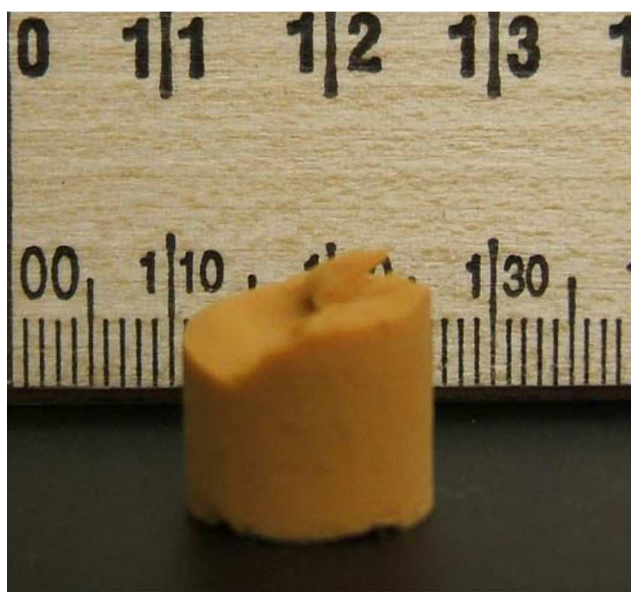


**Fig. 18.** Photograph of  $\text{ZnFe}_2\text{O}_4$  aerogel fabricated using  $\text{Zn}(\text{NO}_3)_2 \cdot 6\text{H}_2\text{O}$  and  $\text{Fe}(\text{NO}_3)_3 \cdot 9\text{H}_2\text{O}$  in 2-propanol. Reproduced from ref. 71 with permission.

The zinc ferrite nanoparticles, surface modified with cetyl trimethylammonium bromide (**11**, Table 2), were applied<sup>74</sup> as an adsorbent for dyes Direct Green 6 (DG6), Direct Red 31 (DR31) and Direct Red 23 (DR23). It was found that dye adsorption onto ZFN-CTAB followed with Langmuir isotherm. It can be concluded that the ZFN-CTAB being as a magnetic adsorbent with high dye adsorption capacity might be a suitable alternative to remove dyes from colored aqueous solutions. Also, nanocrystalline zinc ferrite nanoparticles supported on a silica aerogel porous matrix which differ in size (in the range 4–11 nm) and the inversion degree (from 0.4 to 0.2) as compared to bulk zinc ferrite which has a normal spinel structure.<sup>75</sup> The nanocomposites are superparamagnetic at r.t.; the temperature of the superparamagnetic transition in the samples decreases with the particle size and therefore it is mainly determined by the inversion degree rather than by the particle size, which would give an opposite effect on the blocking temperature. In addition, mixed-metal zinc-containing ferrite-silica adsorbents are also known; thus, ferrite( $\text{Ni}_{0.5}\text{Zn}_{0.5}\text{Fe}_2\text{O}_4$ )-silica aerogel nanocomposite was found to be a ultra-superlight and high-porous material, where the magnetic property of ferrite was held in the aerogel.<sup>76</sup>

Cobalt ferrite is also widespread component in magnetic adsorbents, mainly as aerogels and more rarely hydrogels. Thus, porous cobalt ferrite aerogel catalysts (the crystallite sizes range is between 6.3 and 28.1 nm) were obtained by 1,2-epoxide sol-gel process (by reacting cobalt and iron salts with propylene oxide (similarly to  $\text{ZnFe}_2\text{O}_4$  above) in methanol, dried by supercritical carbon dioxide, and calcined between 200 and 800°C) and investigated in the hydrolysis of 4-nitrophenyl phosphate.<sup>77</sup> The “as-prepared aerogel” surface exhibited M–OH groups that disappear after annealing, which enhances the spinel structure. The catalysts revealed high porosities that decrease as the annealing temperature increases. The catalytic properties of these sol-gel materials were found to be due to the existence of residual surface OH groups that did not undergo condensation. A hybrid hydrogel with  $\text{CoFe}_2\text{O}_4$  NPs as cross-linker agents of carboxymethylcellulose (CMC, **12**, Table 2) polymer was obtained with the aim of testing it as a system for controlled drug release.<sup>78</sup> The NPs were functionalized with (3-aminopropyl)-trimethoxysilane (APTMS) in order to introduce  $\text{NH}_2$  groups on the surface (Figs. 19-21). The hybrid hydrogel combines the magnetic properties of  $\text{CoFe}_2\text{O}_4$  nanoparticles and the behaviors typical of hydrogel to create a new system that overcomes some of the drawbacks of NP use in the field of drug release. This system can be loaded with a large amount of drug and positioned near the target site. In a related report,<sup>79</sup> magnetic hybrid cellulose (**13**, Table 2) aerogels were prepared followed by two steps, firstly, preparation of cellulose hydrogel films from  $\text{LiOH}$ /urea solvent, then  $\text{CoFe}_2\text{O}_4$  nanoparticles were synthesized in the porous structured cellulose scaffolds, which, after being freeze-dried, resulted  $\text{CoFe}_2\text{O}_4$ /cellulose magnetic aerogels. The porosity of the composite aerogels ranged from 78 to 52% with pore size distribution in a few tens of nanometers. These hybrid aerogels showed improved mechanical strength and superparamagnetic properties. Unlike solvent-swollen gels and ferrogels, the magnetic composite aerogels have lightweight, flexibility, and high porosity. Because cellulose is sustainable and readily available in large quantities from plants (wood), this route is suitable for industrial-scale production and may be used with many types of nanoparticles, which will open the application fields of cellulose based functional



materials. As an example, freeze-dried bacterial cellulose nanofibril aerogels on cobalt ferrite basis can be used as templates for making lightweight porous magnetic aerogels, which can be compacted into a stiff magnetic nanopaper.<sup>80</sup>

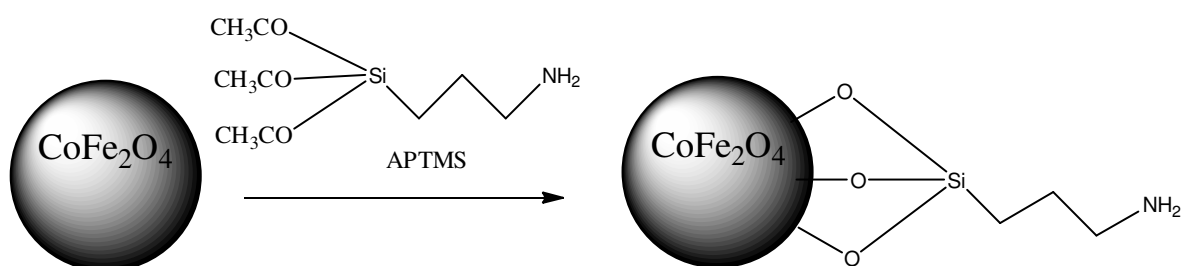


**Fig. 19.** Schematic representation of the functionalization reaction of (3-aminopropyl)-trimethoxysilane (APTMS) with nanoparticle (NP) surface.



**Fig. 20.** Bare (left suspension) and silanized (right suspension) images of CoFe<sub>2</sub>O<sub>4</sub> nanoparticles (0.02 mg/mL, pH 4). The instability of bare nanoparticles is clearly evident. Reproduced from ref. 77 with permission.

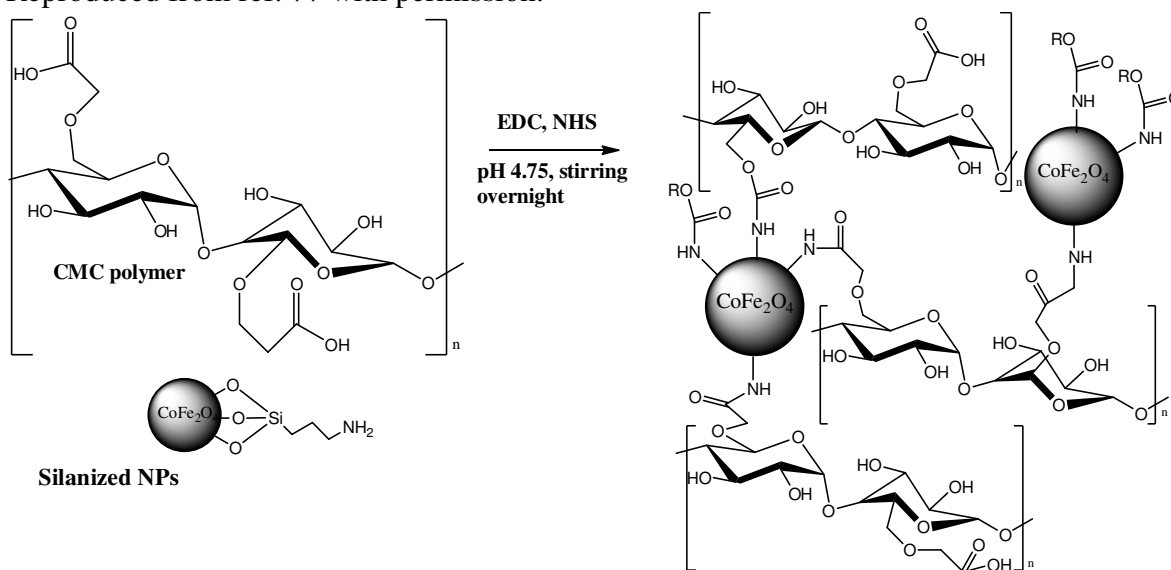


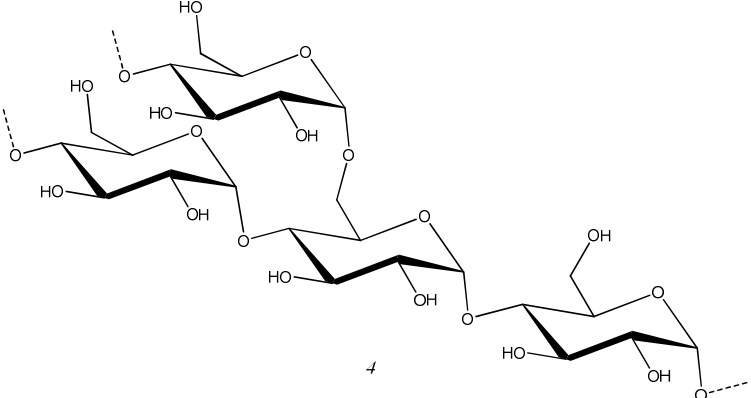
**Fig. 21.** Reaction scheme of the formation of carboxymethylcellulose (CMC) hybrid hydrogels. The reaction involves the formation of an amide bond between the carboxylic groups of CMC and the amine groups of the NP-NH<sub>2</sub> (the cross-linker agent) in the

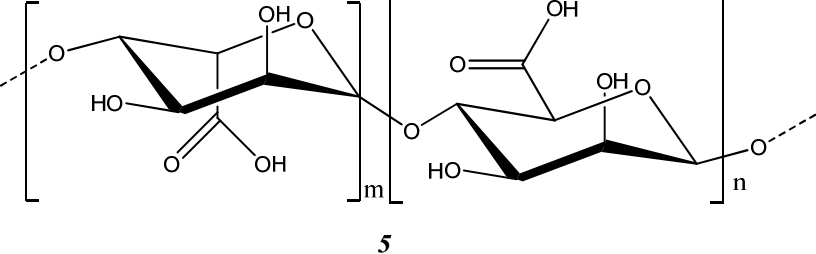
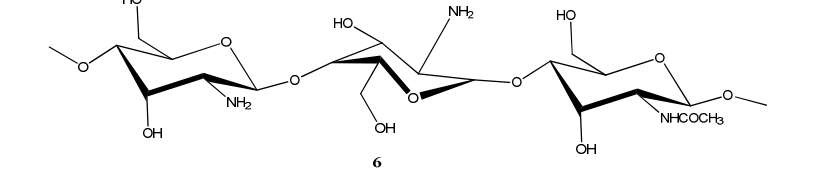
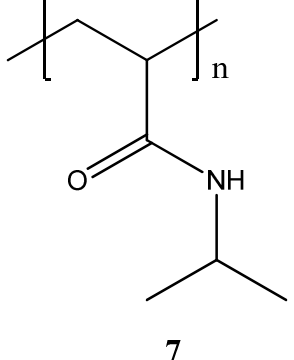
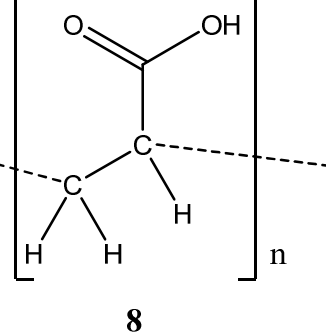
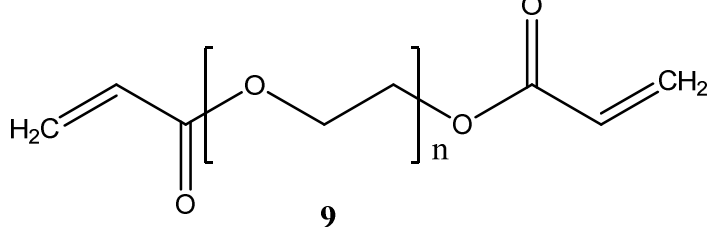
presence of *N*-(3-dimethylaminopropyl)-*N*-ethylcarbodiimidehydrochloride (EDC) and *N*-hydroxysuccinimide (NHS).

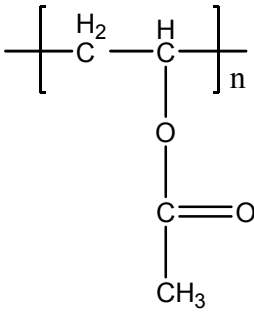
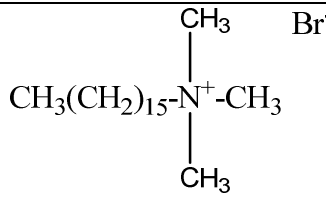
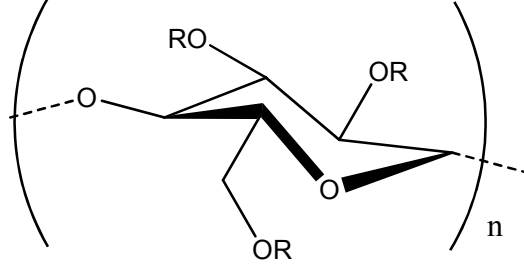
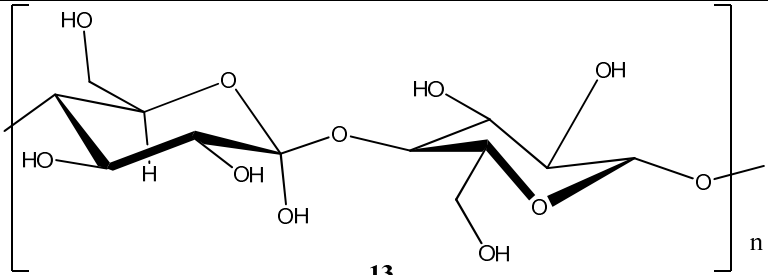
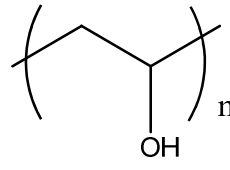
Unusual nanostructures of ferrite basis can be obtained varying  $\text{CoFe}_2\text{O}_4$  concentrations in supports. Thus, magnetic nanocomposite materials consisting of 5 and 10 wt. % ultrasmall stoichiometric  $\text{CoFe}_2\text{O}_4$  nanoparticles in a silica aerogel matrix was synthesized also by the sol-gel method.<sup>81</sup> For the  $\text{CoFe}_2\text{O}_4$ -10 wt. % sample showed many “needle-like” nanostructures that typically have a length of  $\approx 10$  nm and a width of  $\approx 1$  nm, and frequently appear to be attached to nanoparticles. These needle-like nanostructures were observed to contain layers with interlayer spacing  $0.33 \pm 0.1$  nm, which could be consistent with Co silicate hydroxide, a known precursor phase in these nanocomposite materials.

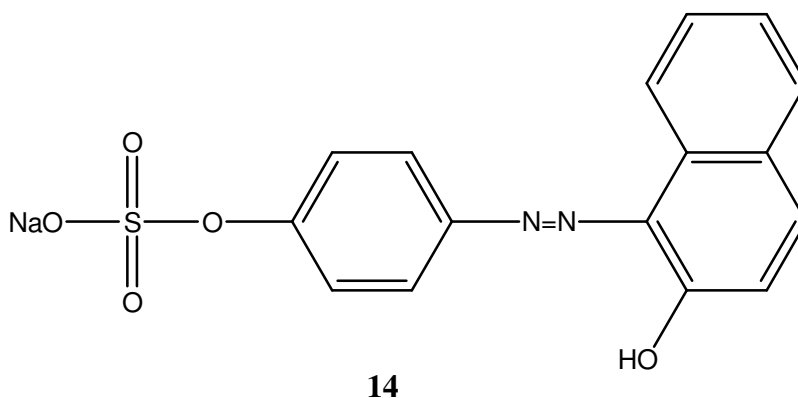
Other ferrite-based magnetic adsorbents are rare. Thus,  $\text{CuFe}_2\text{O}_4$ /activated carbon (mass ratio of 1:1, 1:1.5 and 1:2) magnetic adsorbents, which combined the adsorption features of activated carbon with the magnetic and the excellent catalytic properties of powdered  $\text{CuFe}_2\text{O}_4$ , were developed using a coprecipitation procedure.<sup>82</sup> The prepared magnetic composites can be used to adsorb acid orange II (AO7, **14**) in water and subsequently, easily be separated from the medium by a magnetic technique. The magnetic phase present is spinel copper ferrite and the presence of  $\text{CuFe}_2\text{O}_4$  did not significantly affect the surface area and pore structure of the activated carbon. The composite has much higher catalytic activity than that of activated carbon, attributed to the presence of  $\text{CuFe}_2\text{O}_4$ . Manganese ferrite nanospheres constructed by nanoparticles were synthesized in high yield *via* a general, one-step, and template-free solvothermal method.<sup>83</sup> The resulting sphere-like manganese ferrite particle was a porous structure with a narrow pore-size distribution. Their saturation magnetization is high (maximum saturation magnetization value of the product is 75 emu/g), which shows an excellent ability for magnetic removal of chromium in wastewater.

**Table 2.** Polymers and polysaccharides, used as supports in magnetic sorbents.

Starch	
--------	--

Alginate, also called algin or alginate	 <p style="text-align: center;">5</p>
Chitosan {poly-β-(1,4)-2-amino-2-deoxy-D-glucose}	 <p style="text-align: center;">6</p>
Poly(N-isopropylacrylamide)	 <p style="text-align: center;">7</p>
Polyacrylic acid (PAA)	 <p style="text-align: center;">8</p>
Poly(ethylene glycol)(700) diacrylate, (PEGDA)	 <p style="text-align: center;">9</p>

Polyvinyl acetate (PVAC)	 <p style="text-align: center;"><b>10</b></p>
Cetyl trimethylammonium bromide, CTAB	 <p style="text-align: center;"><b>11</b></p>
Carboxymethylcellulose	 <p style="text-align: center;">R = H or CH<sub>2</sub>CH<sub>2</sub>OH</p> <p style="text-align: center;"><b>12</b></p>
Cellulose	 <p style="text-align: center;"><b>13</b></p>
Polyvinyl alcohol (PVA)	 <p style="text-align: center;"><b>15</b></p>



Acid Orange II

## 6. Magnetic behavior studies

In a predominant number of the reports above, a very frequent statement appears, as an advantage for possible applications of synthesized magnetic adsorbents, that “the adsorbent (or catalyst) can be easily removed from reaction media after adsorption or completion of reactions *via* a simple magnet”. However, we note that, according to our experience, it is not always possible to remove magnetic nanoparticles effectively from solution using classic small magnets, especially in case of ultrasmall particles, well-stabilized in dispersion. Much time is frequently required or the magnet force is insufficient for large volumes of dispersions. Sometimes, stronger magnets need to be applied for their effective separation, when even strong centrifugation does not allow a complete process of precipitate formation. Thus,  $\text{Fe}_3\text{O}_4$  magnetic nanoparticles were used as recoverable adsorbent for lignin removal from aqueous solutions was investigated.<sup>84</sup> Magnetic separation was done using a strong super magnet with 1.4 Tesla magnetic fields (2.5×5×5 cm). Another interesting “magnetic” study was carried out for micron-sized magnetic particles ( $\text{Fe}_3\text{O}_4$ ), dispersed in a polyvinyl alcohol (PVA, **15**, Table 2) hydrogel.<sup>85</sup> This multiferroic ferrogel (Figs. 22-23) combines the elastic properties of PVA gel and the magnetic properties of  $\text{Fe}_3\text{O}_4$  particles. The response of the ferrogel (with  $\text{Fe}_3\text{O}_4$  concentration in the range of 1–10 wt. %) to the application of a static magnetic field (up to a maximum of 40 mT) was studied. It was shown that the extent of deflection depended strongly on the  $\text{Fe}_3\text{O}_4$  content and the magnetic field strength (Fig. 24). For each  $\text{Fe}_3\text{O}_4$  concentration there existed a threshold value of magnetic field strength before large deflection occurred. This implied that the ferrogel system can be used as an ‘on-off’ type transducer. The threshold value decreases with an increase in  $\text{Fe}_3\text{O}_4$  content.



**Fig. 22.** Picture of a ferrogel made of PVA + Fe<sub>3</sub>O<sub>4</sub>. Reproduced from ref. 84 with permission.

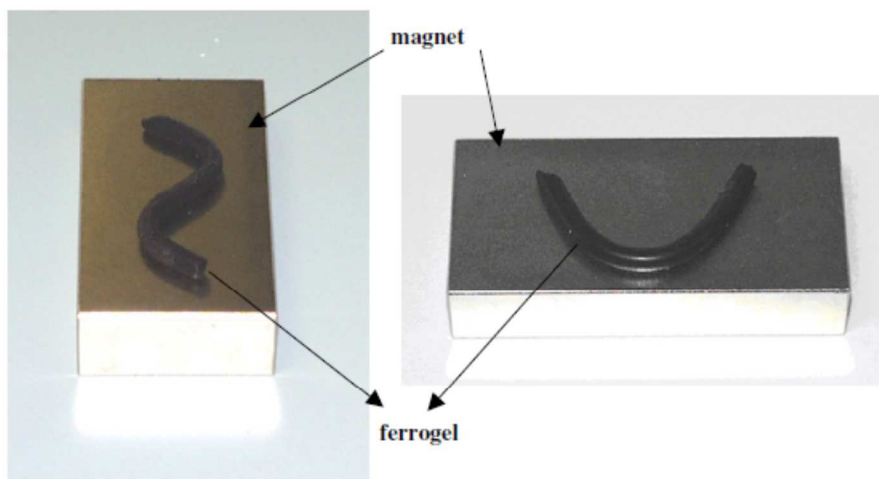


**Fig. 23.** Flexibility of (PVA + Fe<sub>3</sub>O<sub>4</sub>) ferrogel. Reproduced from ref. 84 with permission.



**Fig. 24.** Concentration graded ferrogel, the concentrations are 25, 15 and 3 wt% of iron oxide in the three regions; the highest concentration is closest to the magnet. Reproduced from ref. 84 with permission.

In addition, an interesting finding was observed in case of iron oxide in PEG-containing systems. Thus, the high binding affinity of poly(ethylene glycol)-gallol (PEG-gallol) {PEG, **16**, Table 2} allows freeze drying and re-dispersion of 92-nm iron oxide cores individually stabilized with 9-nm-thick stealth coatings, yielding particle stability for at least 20 months.<sup>86</sup> Fig. 25 shows the prevention of particle agglomeration *even in the presence of a small external magnet*, when the surfactant is used. In all other interactions “suspended MNPs – magnet”, observed in a series of reports, MNPs were attracted by magnets.

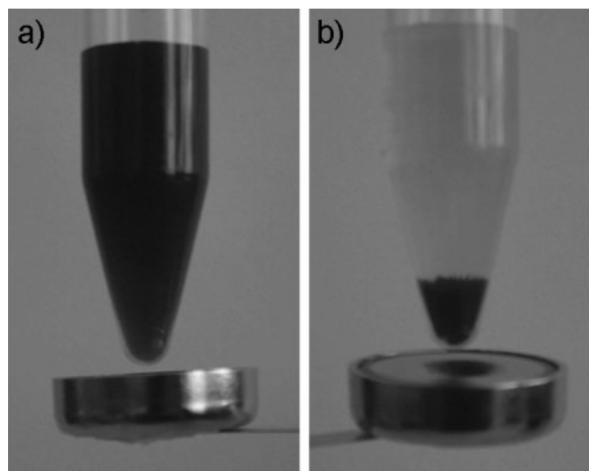


**Fig. 25.** a) The biotin-PEG(3400)-gallol/mPEG(550)-gallol dispersant layer surrounding the iron oxide nanoparticle cores is stable and thick enough to prevent particle agglomeration in the presence of a small external magnet, even after particles have been dispersed in PBS for more than 1 year. B) In the absence of the dispersant layer, iron oxide cores agglomerate and thus sediment instantaneously upon approaching a small external magnet. Reproduced from ref. 85 with permission.

## 7. Environmental applications

Magnetic adsorbents discussed above have a host of applications in distinct areas of science and technology. As it has been observed, they are able to adsorb a series of contaminants in water, for instance trace amounts of Pb(II), Cd(II), Hg(II) and Cu(II) ions in environmental and biological samples, several organic compounds (lignin and various dyes), can separate flavonoids, serve as catalysts, and take part in drug delivery systems for release of drug molecules, as well as in other biomedical applications<sup>87</sup> and, as it is known long ago, in food industry.<sup>88</sup> Symmetric supercapacitors and asymmetric supercapacitors that use carbon xerogels with different porous textures as negative electrode and manganese oxide as positive electrode, are also known.<sup>89</sup>

Due to efficiency in oil sorption, magnetic adsorbents could be useful in a nascent research area: applications of nanomaterials (in particular xerogels and aerogels) in the processes of oil extraction, when oil spills (mixtures of petroleum with water) frequently appear.<sup>90 91 92</sup> This field of technology could have a brilliant future and need to be discussed more in detail. Thus, the technology of producing a magnetic adsorbent for the oil removal from waste water and surface water bodies by the controlled magnetic field, was proposed<sup>93</sup> using magnetite and the absorbent material which is degradable steel slag. The slag consisted of CaO, SiO<sub>2</sub>, Al<sub>2</sub>O<sub>3</sub>, Fe<sub>2</sub>O<sub>3</sub>, MnO, MgO, and Cr<sub>2</sub>O<sub>3</sub>. The weight ratio of slag: magnetite was 1:(1.5-2.0) and optimal particle size of the components was 70-100 microns. Another representative example is 3D macroporous Fe/C nanocomposites {Fe-C-1÷4 (Fig. 26), which {depending on the diameter of polystyrene (PS) microsphere (0.67÷4.2) and pore size (0.35÷3.0)} were investigated as highly selective absorption materials for removing oils from water surface. The macroporous nanocomposites were synthesized by sintering a mixture of closely packed polystyrene microspheres and ferric nitrate precursor

(Fig. 27). These nanocomposites exhibited superhydrophobic and superoleophilic properties without the modification of low-surface-energy chemicals. The macroporous nanocomposites fast and selectively absorbed a wide range of oils and hydrophobic organic solvents on water surface, and the removal of the absorbed oils from the water surface was readily achieved under a magnetic field (Fig. 28). The oil absorption capacity of these nanocomposites was found to be much higher than that of reported  $\text{Fe}_2\text{O}_3@\text{C}$  nanoparticles. Moreover, the nanocomposites still kept highly hydrophobic and oleophilic characteristics after repeatedly removing oils from water surface for many cycles.<sup>94</sup>

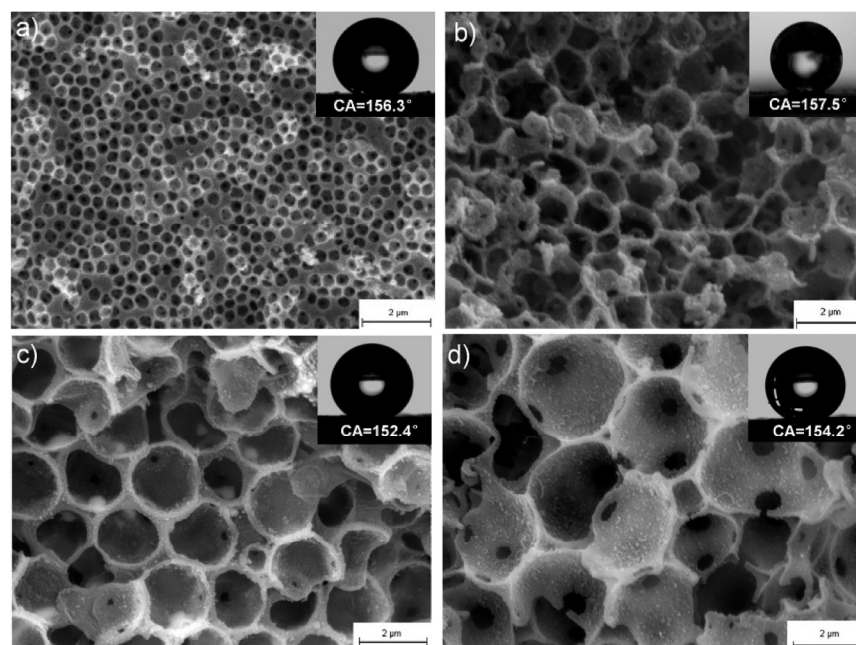


**Fig. 26.** SEM images of (a) Fe/C-1, (b) Fe/C-2, (c) Fe/C-3, and (d) Fe/C-4 samples; inset images are the water contact angles of the corresponding macroporous nanocomposites. Reproduced from ref. 93 with permission.

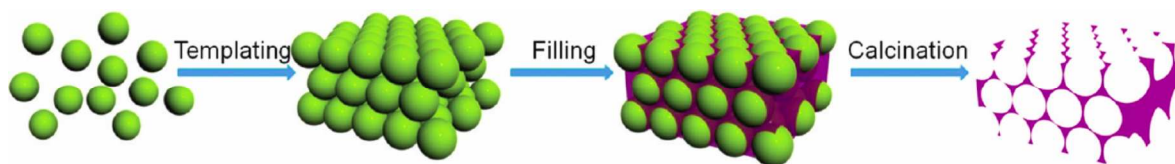


**Fig. 27.** Illustration for the synthesis of three-dimensionally macroporous Fe/C nanocomposites. Reproduced from ref. 93 with permission.



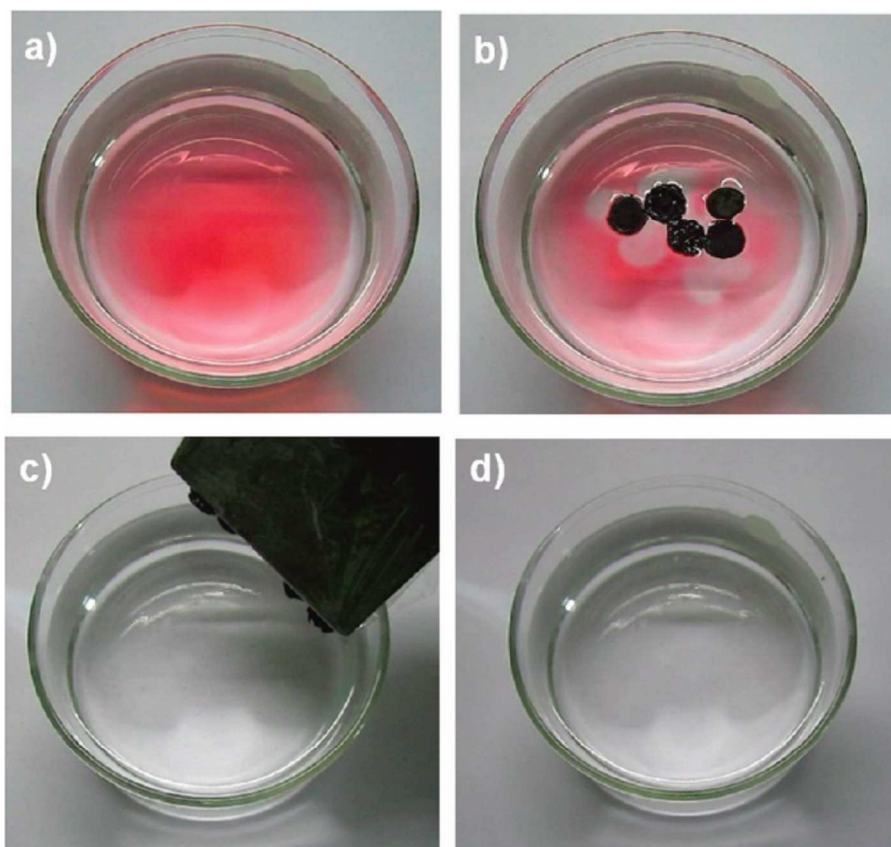


**Fig. 28.** Removal of lubricating oil from water surface by Fe/C-2 sample under magnetic field. The oil was dyed with oil red 24 for clear observation. Reproduced from ref. 93 with permission.

Other iron-carbon composites, magnetic carbon nanotube sponges (M-CNT sponge), porous structures consisting of interconnected CNTs with rich Fe encapsulation, were fabricated by CVD using ferrocene and dichlorobenzene as the precursors. They showed<sup>95</sup> (Fig. 29) high mass sorption capacity for diesel oil reached 56 g/g, corresponding to a volume sorption capacity of 99%. The sponges are mechanically strong and oil can be squeezed out by compression (Fig. 30). They can be recycled using through reclamation by magnetic force and desorption by simple heat treatment. The M-CNT sponges maintain original structure, high capacity, and selectivity after 1000 sorption and reclamation cycles.

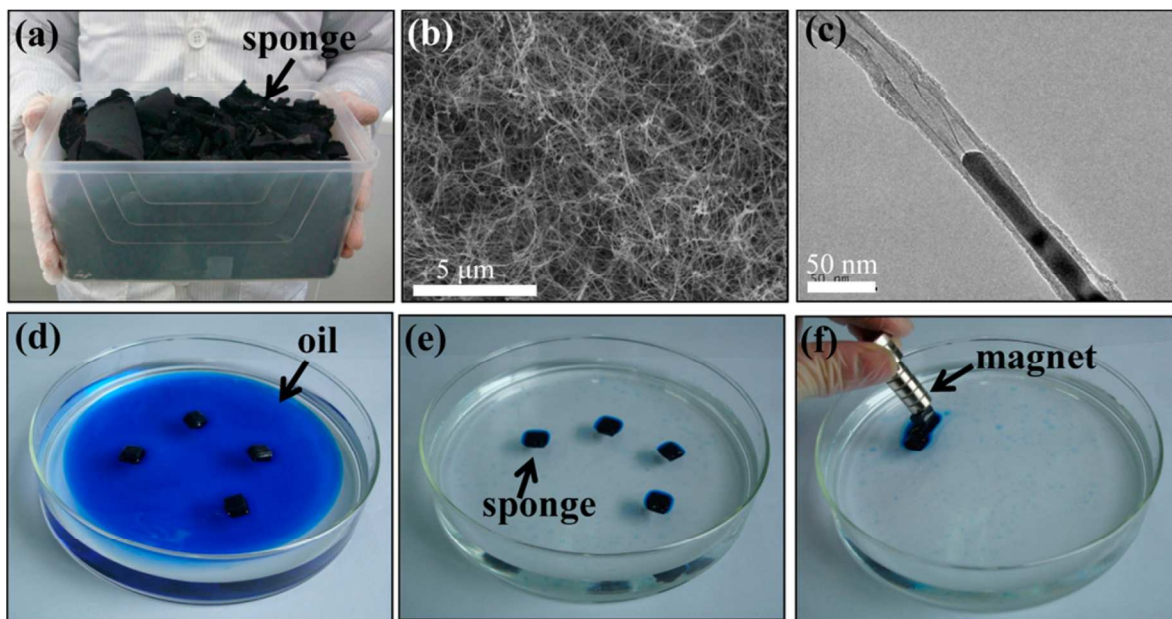


**Fig. 29.** Removal of spilled oil from water surface by M-CNT sponges under magnetic field: (a) Optical image of a box of sponges with volume of approximately 5 L; (b) SEM image of the porous CNT; (c) TEM image of a CNT filled with magnetic Fe nanowires; (d) Oil (dyed blue) spreading on water; four M-CNT sponge blocks have been placed onto the oil; (e) Clean water surface after complete oil absorption by the sponges; (f) Collecting the sponges using a magnet. Reproduced from ref. 94 with permission.

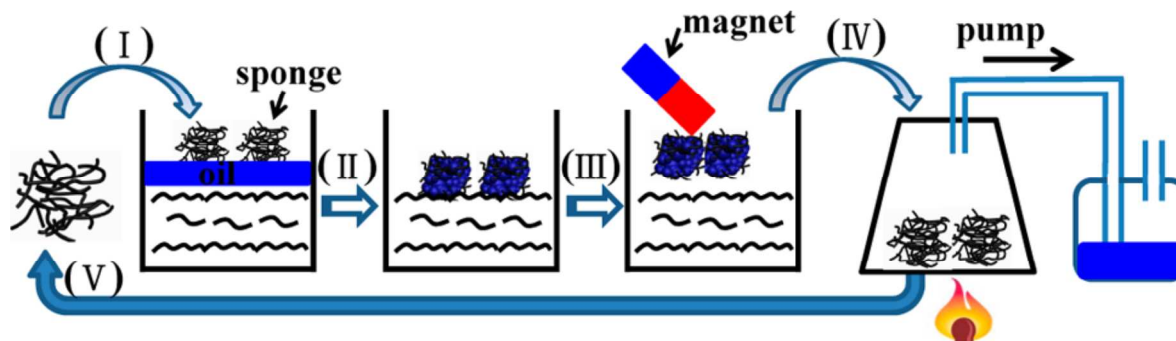


**Fig. 30.** Schematic of the recycling of M-CNT sponges used for spilled oil sorption. (I) sprinkled on the oil; (II) adsorb spilled oil; (III) collected by magnet; (IV) regeneration; (V) reuse. Reproduced from ref. 94 with permission.

A composite material based on commercially available polyurethane foams (PU) functionalized with colloidal superparamagnetic iron oxide nanoparticles (SPIONs) and submicrometer polytetrafluoroethylene (PTFE) particles can efficiently separate oil from water (Fig. 31).<sup>96, 97</sup> It was found that combined functionalization of the PTFE-treated foam surfaces with colloidal iron oxide nanoparticles significantly increases the speed of oil absorption. In addition to the water-repellent and oil-absorbing capabilities, the functionalized foams exhibit also magnetic responsivity. Finally, due to their light weight, they float easily on water. This low-cost process can easily be scaled up to clean large-area

oil spills in water. In a related report,<sup>98</sup> ultralight magnetic  $\text{Fe}_2\text{O}_3/\text{C}$ ,  $\text{Co}/\text{C}$ , and  $\text{Ni}/\text{C}$  foams (with a density  $<5 \text{ mg}\cdot\text{cm}^{-3}$ ) were fabricated (Fig. 32) on the centimeter scale by *pyrolyzing* commercial polyurethane sponge grafted with polyelectrolyte layers based on the corresponding metal acrylate at  $400^\circ\text{C}$ . After modification with low-surface-energy polysiloxane, the ultralight foams showed superhydrophobicity and superoleophilicity, which quickly and selectively absorbed a variety of oils from a polluted water surface under magnetic field. The oil absorption capacity reached 100 times of the foams' own weight, exhibiting one of the highest values among existing absorptive counterparts. In addition, a stable magnetic nanocomposite of collagen and SPIONs was prepared<sup>99</sup> by a simple process utilizing protein wastes from leather industry. This nanocomposite exhibited selective oil absorption and magnetic tracking ability, allowing it to be used in oil removal applications. The environmental sustainability of the oil adsorbed nanobiocomposite was also demonstrated through its conversion into a bifunctional graphitic nanocarbon material via heat treatment.

Discussing economic part of use of magnetic materials for oil clean up using magnetic aerogels, we note that the aerogel in whole is one of the prime candidates for the mitigation of oil spills; however, its high cost is a major inhibiting factor for its widespread adoption. Currently, the typical cost of aerogel produced by supercritical drying is about \$2,870 per kg while the aerogel made from discarded rice husks is reported to cost only \$276 per kg, thereby making the latter a commercially viable proposition. Xerogels are of a lower cost, but their efficiency in oil clean up is lower.

Selected applications of magnetic adsorbents are shown in Table 3.

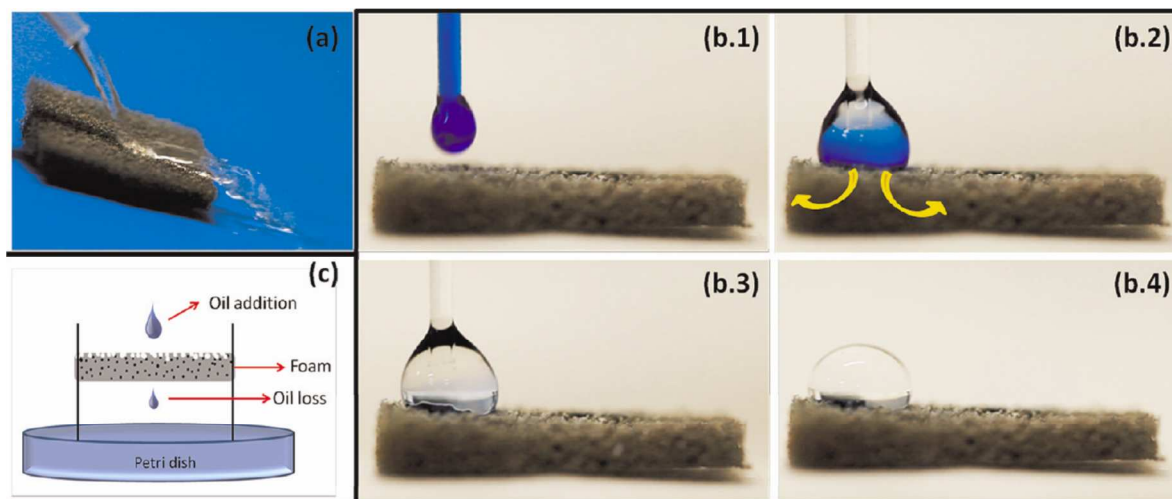


**Fig. 31.** (a) Prolonged water squirt on the PU/NPs/PTFE sample. (b1,2,3,4) Mixed oil (colored with blue dye) and water drop are phase separated, and the oil is immediately absorbed while water remains on the surface. The arrows in (b2) represent the absorption of the oil. Time interval between frames b2 and b3 is less than 1 s. (c) Experimental setup used to determine the foams' oil-absorption capacity. The sample is kept in horizontal position by two needles, and the excess of oil lost through the foam is collected. Reproduced from ref. 95 with permission.

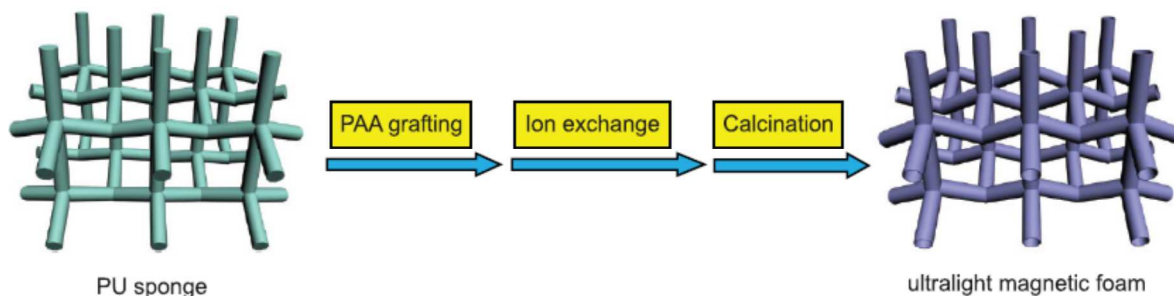


**Fig. 32.** Illustration of the fabrication of ultralight magnetic foams from a polyacrylic acid (PAA)-grafted polyurethane sponge. The foams were constructed from 3D interconnected microtubes having nanoscale wall thickness. Reproduced from ref. 95 with permission.

**Table 3.** Selected applications of magnetic adsorbents.

Adsorbent composition	Application	Reference
<i>Environmental applications</i>		
Sodium alginate-coated $\text{Fe}_3\text{O}_4$ nanoparticles (Alg- $\text{Fe}_3\text{O}_4$ ).	Removal of malachite green from aqueous solutions using batch adsorption technique.	100
Mn-doped maghemite nanoparticles.	Removal of As(V) and As(III) from water.	101
Shell-core structured $\text{Fe}_3\text{O}_4/\text{MnO}_2$ magnetic adsorbent.	Pb(II) removal from aqueous solutions-	102
Carboxymethyl- $\beta$ -cyclodextrin (CM- $\beta$ -CD) polymer modified $\text{Fe}_3\text{O}_4$ nanoparticles (CDpoly-MNPs).	Selective removal of $\text{Pb}^{2+}$ , $\text{Cd}^{2+}$ , $\text{Ni}^{2+}$ from wastewater.	103
Magnetic Fe-Al binary oxide adsorbent.	Chromate removal from aqueous solution with permanent and superconducting magnets (superconducting magnetic separation).	104
Magnetite-porphyrin nanocomposite.	Removal of heavy cations.	105
Polystyrene-magnetite composite.	Solid-phase extraction of uranium(VI) from aqueous nitrate solutions.	106
Cobalt ferrite hollow spheres.	Extraction of uranium(VI) ions from aqueous solutions.	107
$\text{Fe}_3\text{O}_4$ -Embedded graphene oxide.	Removal of methylene blue from aqueous solution.	108

Magnetic-activated coke incorporated with Fe <sub>3</sub> O <sub>4</sub> particles.	Removal of organic materials from 2,4,6-trinitrotoluene red water.	109
Fe <sub>3</sub> O <sub>4</sub> /Au composites.	Extraction of benzo[a]pyrene from aqueous solution.	110
Activated carbon (PAC)/iron oxide composite.	Removal of surfactants from water.	111
Magnetic mesoporous silica microspheres (Fe <sub>3</sub> O <sub>4</sub> @mSiO <sub>2</sub> ).	Fast and convenient enrichment of toxic trace-level microcystin-LR in water.	112
Graphene grafted silica-coated Fe <sub>3</sub> O <sub>4</sub> (Fe <sub>3</sub> O <sub>4</sub> @SiO <sub>2</sub> -G).	Extraction of four neonicotinoid pesticides (thiamethoxam, imidacloprid, acetamiprid and thiacloprid) from pear and tomato samples.	113
<i>Analytical applications</i>		
Fe <sub>3</sub> O <sub>4</sub> /C/PANI (polyaniline) microbowls.	Determination of five pyrethroids in tea drinks (cyhalothrin, beta-cypermethrin, esfenvalerate, permethrin and bifenthrin).	114
Hybrid materials based on magnetic Fe <sub>3</sub> O <sub>4</sub> nanoparticles and synthetic macrocyclic receptor, carboxylato-pillar[5]arene.	Extraction adsorbent for pesticide residue analysis in beverage samples.	115
Magnetite/poly(styrene-divinylbenzene) nanoparticles.	Adsorbent for enrichment-determination of fenitrothion.	116
Adsorbent on the basis of 2,2'-thiodiethanethiol grafted with tetra-Et orthosilicate modified Fe <sub>3</sub> O <sub>4</sub> nanoparticles.	Separation and preconcentration of Hg, Pb, and Cd in environmental and food samples.	117
Ionic liquid-coated Fe <sub>3</sub> O <sub>4</sub> @graphene nanocomposite.	Determination of five nitrobenzene compds.	118
<i>Biomedical applications</i>		
Magnetite/graphene oxide/chitosan (Fe <sub>3</sub> O <sub>4</sub> /GO/CS) composite.	Protein adsorption.	119
Adsorbent on the basis of nickel nanoparticle decorated graphene.	Separation/isolation of His6-tagged recombinant proteins from a complex sample matrix (cell lysate).	120
MWCNTs/Fe <sub>3</sub> O <sub>4</sub> nanocomposite.	Extraction of fluoxetine from human urine samples.	121
Adsorbent on the basis of	Removal of amoxicillin.	122

multi-walled carbon nanotubes and iron oxide nanoparticles.		
Cetyltrimethylammonium bromide adsorbed on the surface of Fe <sub>3</sub> O <sub>4</sub> nanoparticles.	Extraction and preconcentration of ultra-trace amounts of mefenamic acid in biologic fluids.	123

## 8. Conclusions

Magnetic nano- and micro-adsorbents are based on magnetic nanoparticles (mainly iron oxides and ferrites) and supporting agents. The last materials consist of inorganic (carbon, graphene, silica, zeolites) or organic (macromolecules, polysaccharides, polymers, biomolecules) compounds. In the last decade, certain attention is paid to magnetic adsorbents in the form of hydrogels, aerogels,<sup>124</sup> and xerogels due to their numerous applications in removal of heavy metals,<sup>125 126 127 128 129 130 131 132</sup> degradation of dyes and other organic compounds,<sup>133</sup> separation of oil and water mixtures, as well as several biomedical applications.

In these composites, the same chemical compound, being in distinct morphological forms, could play different roles. For example, in the mesoporous composite  $\gamma$ -Fe<sub>2</sub>O<sub>3</sub>/ $\alpha$ -Fe<sub>2</sub>O<sub>3</sub>/CA structures have ferrimagnetic properties due to their  $\gamma$ -Fe<sub>2</sub>O<sub>3</sub> component, and they also have photocatalytic properties because of their antiferromagnetic  $\alpha$ -Fe<sub>2</sub>O<sub>3</sub> component.

Main advantage for possible applications of synthesized magnetic adsorbents, that the adsorbent (or catalyst, if it is used in organic reactions in this role) can be easily removed from reaction media after adsorption or completion of reactions *via* a simple magnet. In combination with polymers, ferrogels combine the elastic properties of polymer gel and the magnetic properties of iron oxide particles. It is expected that applications of magnetic polymer-nanoparticle composites, as well as other described above, will be expanded in near future, in particular for environmental clean up purposes.

## 9. Acknowledgments

OVK and BIK are grateful to the CONACYT-Mexico for financial support.

## 10. References

- <sup>1</sup> Haghi, A. K. *Foundations of Nanotechnology, Volume One: Pore Size in Carbon-Based Nano-Adsorbents: 1* (AAP Research Notes on Nanoscience and Nanotechnology). Apple Academic Press, 1 edition, **2014**, 278 pp.
- <sup>2</sup> Nasreen, S.; Rafique, U. *Novel Adsorbents for Removal of Aqueous Pollutants: Nano-Synthesis: Silica and Alumina: Meso and Nano-Adsorbents*, LAP LAMBERT Academic Publishing, **2012**, 96 pp.
- <sup>3</sup> Reisner, D.E.; T. Pradeep, T. *Aquananotechnology: Global Prospects*, CRC Press, **2014**, 863 pp.

- <sup>4</sup> Hu, A.; Apblett, A. *Nanotechnology for Water Treatment and Purification (Lecture Notes in Nanoscale Science and Technology)*, Springer, **2014**, 373 pp.
- <sup>5</sup> Aditya, D.; Rohan, P.; Suresh, G. Nano-adsorbents for Wastewater Treatment: A Review. *Research Journal of Chemistry and Environment*, **2011**, 15 (2), 1033
- <sup>6</sup> Sharma, Y.C.; Srivastava, V.; Singh, V.K.; Kaul, S.N.; Weng, C.H. Nano-adsorbents for the removal of metallic pollutants from water and wastewater. *Environ Technol.* **2009**, 30(6), 583-609.
- <sup>7</sup> Khajeh, M.; Laurent, S.; Dastafkan, K. Nano-adsorbents: Classification, Preparation, and Applications (with Emphasis on Aqueous Media). *Chem. Rev.*, **2013**, 113 (10), 7728–7768. <http://pubs.acs.org/doi/abs/10.1021/cr400086v>
- <sup>8</sup> Mosiniewicz-Szablewska, E.; Safarikova, M.; Safarik, I. Magnetically modified biological materials as perspective adsorbents for large-scale magnetic separation processes. *Horizons in World Physics*, **2010**, 266(Applied Physics in the 21st Century), 301-318.
- <sup>9</sup> Liu, S.; Luo, X.; Zhou, J. Magnetic Responsive Cellulose Nanocomposites and Their Applications. In: *Cellulose - Medical, Pharmaceutical and Electronic Applications*, book edited by Theo van de Ven and Louis Godbout, InTech, **2013**.
- <sup>10</sup> Franzreb, M.; Siemann-Herzberg, M.; Hobley, T.J.; Thomas, O.R.T. Protein purification using magnetic adsorbent particles. *Appl. Microbiol. Biotechnol.*, **2006**, 70, 505–516.
- <sup>11</sup> Kasemann, R.; Schmitd, H. K. A new type of a sol-gel derived inorganic-organic nanocomposite. *Materials Research Society, Symp. Proc.*, **1994**, 346, 915-921.
- <sup>12</sup> Gan, Y. X. Structural assessment of nanocomposites. *Micron*, **2012**, 43, 782-817.
- <sup>13</sup> Della Santina Mohallem, N.; Batista Silva, J.; Tacchi Nascimento, G.L.; Guimarães, V.L. Study of Multifunctional Nanocomposites Formed by Cobalt Ferrite Dispersed in a Silica Matrix Prepared by Sol-Gel Process. In: *Nanocomposites - New Trends and Developments*, book edited by Ebrahimi, F. InTech, **2012**.
- <sup>14</sup> Cotet, L.C.; Fort, C.I.; Danciu, V.; Maicaneanu, A. Cu and Cd Adsorption on Carbon Aerogel and Xerogel. *E3S Web of Conferences*, **2013**, 1, 25007.
- <sup>15</sup> Nelcy Della Santina Mohallem, Juliana Batista Silva, Gabriel L. Tacchi Nascimento and Victor L. Guimarães. Study of Multifunctional Nanocomposites Formed by Cobalt Ferrite Dispersed in a Silica Matrix Prepared by Sol-Gel Process. In: *Nanocomposites - New Trends and Developments*, book edited by Farzad Ebrahimi, InTech, **2012**.
- <sup>16</sup> Gurav, J.L.; Jung, I.-K.; Park, H.-H.; Kang, E.S.; Nadargi, D.Y. Silica Aerogel: Synthesis and Applications. *Journal of Nanomaterials*, **2010**, Article ID 409310, 11 pp.
- <sup>17</sup> Liu, Z.; Wang, H.; Liu, C.; Jiang, Y.; Yu, G.; Mu, X.; Wang, X. Magnetic cellulose-chitosan hydrogels prepared from ionic liquids as reusable adsorbent for removal of heavy metal ions. *Chem. Commun.*, **2012**, 48, 7350-7352.
- <sup>18</sup> Su Kyung Suh; Chapin, S.C.; Alan Hatton, T.; Doyle, P.S. Synthesis of magnetic hydrogel microparticles for bioassays and tweezer manipulation in microwells. *Microfluid Nanofluid*, **2012**, 13, 665–674.
- <sup>19</sup> Feng Xu; Chung-an Max Wu; Venkatakrishnan Rengarajan; Thomas Dylan Finley; Hasan Onur Keles; Yuree Sung; Baoqiang Li; Umut Atakan Gurkan; Utkan Demirci. Three-Dimensional Magnetic Assembly of Microscale Hydrogels. *Adv. Mater.* **2011**, 23, 4254–4260.

- <sup>20</sup> Vashist, A.; Ahmad, S. Hydrogels: Smart Materials for Drug Delivery. *Oriental J. Chem.*, **2013**, *29* (3), 861-870.
- <sup>21</sup> Zrínyi, M.; Barsi, L.; Büki, A. Ferrogel: a new magneto-controlled elastic medium. *Polymer Gels and Networks*, **1997**, *5* (5), 415–427.
- <sup>22</sup> Venkatesan, M.; Pazhanisamy, P. Synthesis and Dye Adsorption Studies of Poly (N-tert-butylacrylamide-co-acrylamide/Maleic acid) Ferrogel. *Ind. J. Res.*, **2014**, *3* (5), 20-22.
- <sup>23</sup> Petrova, T.M.; Fachikov, L.; Hristov, J. The Magnetite as Adsorbent for Some Hazardous Species from Aqueous Solutions: a Review. *International Review of Chemical Engineering (I.R.E.C.H.E.)*, **2012**, *3* (2), 134-152.
- <sup>24</sup> Zhou, S.; Wang, D.; Sun, H.; Chen, J.; Wu, S.; Na, P. Synthesis, Characterization, and Adsorptive Properties of Magnetic Cellulose Nanocomposites for Arsenic Removal. *Water, Air, & Soil Pollution*, **2014**, *225*(5), 1-13.
- <sup>25</sup> Yang, X.; Shen, X.; Jing, M.; Liu, R.; Lu, Y.; Xiang, J. Removal of heavy metals and dyes by supported nano zero-valent iron on barium ferrite microfibers. *Journal of Nanoscience and Nanotechnology*, **2014**, *14*(7), 5251-5257.
- <sup>26</sup> Jabeen, H.; Kemp, K. C.; Chandra, V. Synthesis of nano zerovalent iron nanoparticles - Graphene composite for the treatment of lead contaminated water. *Journal of Environmental Management*, **2013**, *130*, 429-435.
- <sup>27</sup> Wang, Z.; Liu, X.; Lv, M.; Meng, J. A new kind of mesoporous Fe<sub>7</sub>Co<sub>3</sub>/carbon nanocomposite and its application as magnetically separable adsorber. *Materials Letters*, **2010**, *64*(10), 1219-1221.
- <sup>28</sup> Wang, Z.; Liu, R.; Zhao, F.; Liu, X.; Lv, M.; Meng, J. Facile Synthesis of Porous Fe<sub>7</sub>Co<sub>3</sub>/Carbon Nanocomposites and Their Applications as Magnetically Separable Adsorber and Catalyst Support. *Langmuir*, **2010**, *26*(12), 10135-10140.
- <sup>29</sup> Costa, D. A. S.; Mambrini, R. V.; Fernandez-Outon, L. E.; Macedo, W. A. A.; Moura, Flavia C. C. Magnetic adsorbent based on cobalt core nanoparticles coated with carbon filaments and nanotubes produced by chemical vapor deposition with ethanol. *Chemical Engineering Journal*, **2013**, *229*, 35-41.
- <sup>30</sup> Jiang, Z.; Xie, J.; Jiang, D.; Yan, Z.; Jing, J.; Liu, D. Enhanced adsorption of hydroxyl contained/anionic dyes on non functionalized Ni@SiO<sub>2</sub> core-shell nanoparticles: Kinetic and thermodynamic profile. *Applied Surface Science*, **2014**, *292*, 301-310.
- <sup>31</sup> Wang, Y.; Zhao, G.; Chai, S.; Zhao, H.; Wang, Y. Three-Dimensional Homogeneous Ferrite-Carbon Aerogel: One Pot Fabrication and Enhanced Electro-Fenton Reactivity. *ACS Appl. Mater. Interfaces*, **2013**, *5*, 842–852.
- <sup>32</sup> Hsu, S.H.; Lin, Y.-F.; Chung, T.W.; Wei, T.-Y.; Lu, S.-Y.; Tunga, K.-L.; Liu, K.-T. Mesoporous carbon aerogel membrane for phospholipid removal from *Jatropha curcas* oil. *Separation and Purification Technology*, **2013**, *109*, 129–134.
- <sup>33</sup> Lin, Y.-F.; Chang, C.Y. Magnetic mesoporous iron oxide/carbon aerogel photocatalysts with adsorption ability for organic dye removal. *RSC Adv.*, **2014**, *4*, 28628–28631.
- <sup>34</sup> Wu, X.; Jia, W. Biomass-derived multifunctional magnetite carbon aerogel nanocomposites for recyclable sequestration of ionizable aromatic organic pollutants. *Chem. Engin. J.*, **2014**, *245*, 210-216.
- <sup>35</sup> Cong, H.-P.; Ren, X.-C.; Wang, P.; Yu, S.-H. Macroscopic Multifunctional Graphene-Based Hydrogels and Aerogels by a Metal Ion Induced Self-Assembly Process. *ACS Nano*, **2012**, *6*(3), 2693-2703.



- <sup>36</sup> Cannas, C.; Casula, M.F.; Concas, G.; Corrias, A.; Gatteschi, D.; Falqui, A.; Musinu, A.; Sangregorioc, C.; Spano, G. Magnetic properties of  $\gamma$ -Fe<sub>2</sub>O<sub>3</sub>-SiO<sub>2</sub> aerogel and xerogel nanocomposite materials. *J. Mater. Chem.*, **2001**, *11*, 3180–3187.
- <sup>37</sup> Fernández van Raap, M.B.; Sánchez, F.H.; Rodríguez Torres, C.E.; Casas, L.; Roig, A.; Molins, E. Detailed magnetic dynamic behaviour of nanocomposite iron oxide aerogels. *J. Phys.: Condens. Matter*, **2005**, *17*, 6519–6531.
- <sup>38</sup> Lee, J.S.; Lee, E.J.; Hwang, H.J. Synthesis of Fe<sub>3</sub>O<sub>4</sub>-coated silica aerogel nanocomposites. *Trans. Nonferrous Met. Soc. China*, **2012**, *22*, s702–s706.
- <sup>39</sup> Zhang, B.; Xing, J.M.; Lang, Y.Q.; Liu, H.Z. Synthesis of amino-silane modified magnetic silica adsorbents and application for adsorption of flavonoids from *Glycyrrhiza uralensis* Fisch. *Sci. China Ser. B - Chem.*, **2008**, *51* (2), 145-151.
- <sup>40</sup> Oxana V. Kharissova, H. V. Rasika Dias, Boris I. Kharisov, Betsabee Olvera Pérez, Victor M. Jiménez Pérez. The greener synthesis of nanoparticles. *Trends in Biotechnology*, **2013**, *31*(4), 240-248.
- <sup>41</sup> Bagheri, H.; Afkhami, A.; Saber-Tehrani, M.; Khoshshafar, H. Preparation and characterization of magnetic nanocomposite of Schiff base/silica/magnetite as a preconcentration phase for the trace determination of heavy metal ions in water, food and biological samples using atomic absorption spectrometry. *Talanta*, **2012**, *97*, 87–95.
- <sup>42</sup> Wang, S.; Peng, Y. Natural zeolites as effective adsorbents in water and wastewater treatment. *Chemical Engineering Journal*, **2010**, *156* (1), 11–24.
- <sup>43</sup> White, J.C.; Dutta, P.K. Assembly of Nanoparticles in Zeolite Y for the Photocatalytic Generation of Hydrogen from Water. *J. Phys. Chem. C*, **2011**, *115*, 2938–2947.
- <sup>44</sup> Shameli, K.; Bin Ahmad, M.; Zargar, M.; Wan Md Zin Wan Yunus; Azowa Ibrahim, N. Fabrication of silver nanoparticles doped in the zeolite framework and antibacterial activity. *Int. J. Nanomedicine*. **2011**, *6*, 331–341.
- <sup>45</sup> Kulshreshtha, S.K.; Vijayalakshmi, R.; Sudarsan, V.; Salunke, H.G.; Bhargava, S.C. Iron oxide nanoparticles in NaA zeolite cages. *Solid State Sciences*, **2013**, *21*, 44–50.
- <sup>46</sup> Ulucan, K.; Noberi, C.; Coskun, T.; Bulent Ustundag, C.; Debik, E.; Kaya, C. Disinfection By-Products Removal by Nanoparticles Sintered in Zeolite. *Journal of Clean Energy Technologies*, **2013**, *1* (2), 120-123.
- <sup>47</sup> Salem Attia, T.M.; Lin Hu, X.; Qiang Yin, D. Synthesized magnetic nanoparticles coated zeolite for the adsorption of pharmaceutical compounds from aqueous solution using batch and column studies. *Chemosphere*, **2013**, *93* (9), 2076–2085.
- <sup>48</sup> Fungaro, D.A.; Yamaura, M.; Craesmeyer, G.R. Uranium Removal from Aqueous Solution by Zeolite from Fly Ash-Iron Oxide Magnetic Nanocomposite. *International Review of Chemical Engineering (I.RE.C.H.E.)*, **2012**, *4* (3), 353-358.
- <sup>49</sup> Yamaura, M.; Alves Fungaro, M. Synthesis and characterization of magnetic adsorbent prepared by magnetite nanoparticles and zeolite from coal fly ash. *Journal of Materials Science*, **2013**, *48* (14), 5093-5101.
- <sup>50</sup> Bosinceanu, R.; Sulitanu, N. Synthesis and characterization of FeO(OH)/Fe<sub>3</sub>O<sub>4</sub> nanoparticles encapsulated in zeolite matrix. *J. Optoelectr. Adv. Mater.*, **2008**, *10* (12), 3482–3486.
- <sup>51</sup> Pergher, S.B.C.; Oliveira, L.C.; Smaniotto, A.; Petkowicz, D.I. Magnetic zeolites for removal of metals in water. *Quím. Nova*, **2005**, *28* (5), 751-755.

- <sup>52</sup> Chen, X.; Lam, K.F.; Zhang, Q.; Pan, B.; Arruebo, M.; Yeung, K.L. Synthesis of Highly Selective Magnetic Mesoporous Adsorbent. *J. Phys. Chem. C*, **2009**, *113*, 9804–9813.
- <sup>53</sup> Yang, Q.; Jiang, Y.; Li, X.; Yang, Y.; Hu, L. Magnetic-supported cucurbituril: A recyclable adsorbent for the removal of humic acid from simulated water. *Bull. Mater. Sci.*, **2014**, *37* (5), 1167–1174.
- <sup>54</sup> Masson, E.; Ling, X.; Joseph, R.; Kyeremeh-Mensah, L.; Lu, X. Cucurbituril chemistry: a tale of supramolecular success. *RSC Adv.*, **2012**, *2*, 1213–1247.
- <sup>55</sup> Konne, J.L.; Okpara, K. Remediation of Nickel from Crude Oil Obtained from Bomu Oil Field Using Cassava Waste Water Starch Stabilized Magnetic Nanoparticles. *Energy and Environment Research*, **2014**, *4* (1), 25–31.
- <sup>56</sup> Zhu, H.; Fu, Y.; Jiang, R.; Yao, J.; Xiao, L.; Zeng, G. Optimization of Copper(II) Adsorption onto Novel Magnetic Calcium Alginate/Maghemite Hydrogel Beads Using Response Surface Methodology. *Ind. Eng. Chem. Res.* **2014**, *53*, 4059–4066.
- <sup>57</sup> El-Sherbiny, I.M.; Smyth, H.D.C. Smart Magnetically Responsive Hydrogel Nanoparticles Prepared by a Novel Aerosol-Assisted Method for Biomedical and Drug Delivery Applications. *Journal of Nanomaterials*, **2011**, Article ID 910539, 13 pp.
- <sup>58</sup> Kyzas, G.Z.; Deliyanni, E.A. Mercury(II) Removal with Modified Magnetic Chitosan Adsorbents. *Molecules*, **2013**, *18*, 6193–6214.
- <sup>59</sup> Paneva, D.; Stoilova, O.; Manolova, N.; Rashkov, I. Magnetic hydrogel beads based on chitosan. *e-Polymers*, **2004**, *4* (1), 673–683.
- <sup>60</sup> Huang, K.S.; Wang, C.-Y.; Yang, C.-H.; Mihai Grumezescu, A.; Lin, Y.-S.; Kung, C.P.; Lin, I.-Y.; Chang, Y.-C.; Weng, W.-J.; Wang, W.-T. Synthesis and Characterization of Oil-Chitosan Composite Spheres. *Molecules*, **2013**, *18*, 5749–5760.
- <sup>61</sup> Šafarik, I.; Ptackov, L.; Šafarikova, M. Laboratory of Biochemistry and Microbiology, Institute of Landscape Large-scale separation of magnetic bioaffinity adsorbents. *Biotechnology Letters*, **2001**, *23*, 1953–1956.
- <sup>62</sup> Satarkar, N.S.; Zach Hilt, J. Magnetic hydrogel nanocomposites for remote controlled pulsatile drug release. *Journal of Controlled Release*, **2008**, *130*, 246–251.
- <sup>63</sup> Satarkar, N.S.; Zhang, W.; Eitel, R.E.; Zach Hilt, J. Magnetic hydrogel nanocomposites as remote controlled microfluidic valves. *Lab Chip*, **2009**, *9*, 1773–1779.
- <sup>64</sup> Tabatabaei, S.N.; Lapointe, J.; Martel, S. Magnetic Nanoparticles Encapsulated in Hydrogel as Hyperthermic Actuators for Microrobots Designed to Operate in the Vascular Network. *Intelligent Robots and Systems (IROS 2009. IEEE/RSJ International Conference on)*, **2009**, 546–551. DOI: 10.1109/IROS.2009.5354162.
- <sup>65</sup> Razmjou, A.; Reza Barati, M.; Simon, G.P.; Suzuki, K.; Wang, H. Fast Deswelling of Nanocomposite Polymer Hydrogels via Magnetic Field-Induced Heating for Emerging FO Desalination. *Environ. Sci. Technol.* **2013**, *47*, 6297–630.
- <sup>66</sup> Liao, M.-H.; Chen, D.-H. Preparation and characterization of a novel magnetic nano-adsorbent. *J. Mater. Chem.*, **2002**, *12*, 3654–3659.
- <sup>67</sup> Hwang, D.K.; Dendukuri, D.; Doyle, P.S. Microfluidic-based synthesis of non-spherical magnetic hydrogel microparticles. *Lab Chip*, **2008**, *8*, 1640–1647.
- <sup>68</sup> Pavia-Sanders, A.; Zhang, S.; Flores, J.A.; Sanders, J.E.; Raymond, J.E.; Wooley, K.L. Robust Magnetic/Polymer Hybrid Nanoparticles Designed for Crude Oil Entrapment and Recovery in Aqueous Environments. *ACS Nano*, **2013**, *7* (9), 7552–7561.

- <sup>69</sup> Tseng, J.-Y.; Chang, C.-Y.; Chen, Y.H.; Chang, C.F.; Chiang, P.C. Synthesis of micro-size magnetic polymer adsorbent and its application for the removal of Cu(II) ion. *Colloids and Surfaces A: Physicochem. Eng. Aspects*, **2007**, *295*, 209–216.
- <sup>70</sup> Thanikaivelan, P.; Narayanan, N.T.; Pradhan, B.K.; Ajayan, P.M. Collagen based magnetic nanocomposites for oil removal applications. *Sci. Reports*, **2012**, *2*, 230, 7 pp.
- <sup>71</sup> Hamdeh, H. H.; Ho, J. C.; Oliver, S. A.; Willey, R. J.; Oliveri, G.; Busca, G. Magnetic properties of partially-inverted zinc ferrite aerogel powders. *Journal of Applied Physics*, **1997**, *81*, 1851.
- <sup>72</sup> Brown, P.; Hope-Weeks, L.J. The synthesis and characterization of zinc ferrite aerogels prepared by epoxide addition. *J. Sol-Gel Sci. Technol.* **2009**, *51*, 238–243.
- <sup>73</sup> Makovec, D.; Drogenik, M. Non-stoichiometric zinc-ferrite spinel nanoparticles. *J. Nanopart. Res.*, **2008**, *10*, 131–141.
- <sup>74</sup> Mahmoodi, D.M.; Abdi, J.; Bastani, D. Direct dyes removal using modified magnetic ferrite nanoparticle. *Journal of Environmental Health Science & Engineering*, **2014**, *12*, 96, 10 pp.
- <sup>75</sup> Bullita, S.; Casu, A.; Casula, M. F.; Concas, G.; Congiu, F.; Corrias, A.; Falqui, A.; Lochea, D.; Marrasa, C. ZnFe<sub>2</sub>O<sub>4</sub> nanoparticles dispersed in a highly porous silica aerogel matrix: a magnetic study. *Phys. Chem. Chem. Phys.*, **2014**, *16*, 4843–4852.
- <sup>76</sup> Katagiri, N.; Adachi, N.; Ota, T. Preparation of a magnetic aerogel from ferrite-silica nanocomposite. *ChemXpress*, **2014**, *4*(2), 221–227.
- <sup>77</sup> Akl, J.; Ghaddar, T.; Ghanem, A.; El-Rassy, H. Cobalt ferrite aerogels by epoxide sol-gel addition: Efficient catalysts for the hydrolysis of 4-nitrophenyl phosphate. *Journal of Molecular Catalysis A: Chemical*, **2009**, *312*, 18–22.
- <sup>78</sup> Giani, G.; Fedi, S.; Barbucci, R. Hybrid Magnetic Hydrogel: A Potential System for Controlled Drug Delivery by Means of Alternating Magnetic Fields. *Polymers*, **2012**, *4*, 1157–1169.
- <sup>79</sup> Liu, S.; Yan, Q.; Tao, D.; Yu, T.; Liu, X. Highly flexible magnetic composite aerogels prepared by using cellulose nanofibril networks as templates. *Carbohydrate Polymers*, **2012**, *89*, 551–557.
- <sup>80</sup> Olsson, R.T.; Azizi Samir, M.A.S.; Salazar-Alvarez, G.; Belova, L.; Strom, V.; Berglund, L.A.; Ikkala, O.; Nogues, J.; Gedde, U.W. Making flexible magnetic aerogels and stiff magnetic nanopaper using cellulose nanofibrils as templates. *Nature Nanotechnol.*, **2010**, *5*, 584–588.
- <sup>81</sup> Falqui, A.; Corrias, A.; Wang, P.; Snoeck, E.; Mountjoy, G. A Transmission Electron Microscopy Study of CoFe<sub>2</sub>O<sub>4</sub> Ferrite Nanoparticles in Silica Aerogel Matrix Using HREM and STEM Imaging and EDX Spectroscopy and EELS. *Microsc. Microanal.*, **2010**, *16*, 200–209.
- <sup>82</sup> Zhang, G.; Qu, J.; Liu, J.; Cooper, A.T.; Wu, R. CuFe<sub>2</sub>O<sub>4</sub>/activated carbon composite: A novel magnetic adsorbent for the removal of acid orange II and catalytic regeneration. *Chemosphere*, **2007**, *68*, 1058–1066.
- <sup>83</sup> Yang, L.-X.; Wang, F.; Meng, Y.-F.; Tang, Q.-H.; Liu, Z.-Q. Fabrication and Characterization of Manganese Ferrite Nanospheres as a Magnetic Adsorbent of Chromium. *Journal of Nanomaterials*, **2013**, Article ID 293464, 5 pp.

- <sup>84</sup> Mostashari, S.M.; Shariati, S.; Manoochehri, M. Lignin removal from aqueous solutions using Fe<sub>3</sub>O<sub>4</sub> magnetic nanoparticles as recoverable adsorbent. *Cellulose Chem. Technol.*, **2013**, *47* (9-10), 727-734.
- <sup>85</sup> Ramanujan, R.V.; Lao, L.L. The mechanical behavior of smart magnet-hydrogel composites. *Smart Mater. Struct.*, **2006**, *15*, 952-956.
- <sup>86</sup> Amstad, E.; Zurcher, S.; Mashaghi, A.; Wong, J.Y.; Textor, M.; Reimhult, E. Surface Functionalization of Single Superparamagnetic Iron Oxide Nanoparticles for Targeted Magnetic Resonance Imaging. *Small*, **2009**, *5* (11), 1334-1342.
- <sup>87</sup> Li, Y.; Huang, G.; Zhang, X.; Li, B.; Chen, Y.; Lu, T.; Lu, T.J.; Xu, F. Magnetic Hydrogels and Their Potential Biomedical Applications. *Adv. Funct. Mater.* **2013**, *23*, 660-672.
- <sup>88</sup> Dixon, D.R. Magnetic adsorbents: Properties and applications. *Journal of Chemical Technology and Biotechnology*, **1980**, *30* (1), 572-578.
- <sup>89</sup> Lufrano, F.; Staiti, P.; Calvo, E.G.; Juárez-Pérez, E.J.; Menéndez, J.A.; Arenillas, A. Carbon Xerogel and Manganese Oxide Capacitive Materials for Advanced Supercapacitors. *Int. J. Electrochem. Sci.*, **2011**, *6*, 596-612.
- <sup>90</sup> Mahajan, Y.R. Nanotechnology-based solutions for oil spills. Nanotechnology-based Solutions for Oil Spills. *Nanotech Insights*, **2011**, *2* (1), <http://www.nanowerk.com/spotlight/spotid=20215.php>
- <sup>91</sup> Viswanathan, T. Use of magnetic carbon composites from renewable resource materials for oil spill clean up and recovery. WO 2011008315 A1, **2011**.
- <sup>92</sup> Apblett, A.W.; Al-Fadul, S.M.; Trad, T. Removal of petrochemicals from water using magnetic filtration. The 8th International Petroleum Environmental Conference, November 6-9, **2001**, Houston, TX. [http://ipecc.utulsa.edu/Conf2001/apblett\\_101.pdf](http://ipecc.utulsa.edu/Conf2001/apblett_101.pdf).
- <sup>93</sup> Rubanov, Yu.K.; Tokach, Yu.F.; Kustitckaya, O.E.; Vezentcev, A.I. Intensification of Adsorption Processes of Hydrocarbons Extraction from Aqueous Media by the Controlled Magnetic Field. *Middle-East Journal of Scientific Research*, **2013**, *18* (10), 1473-1478.
- <sup>94</sup> Chu, Y.; Pan, Q. Three-Dimensionally Macroporous Fe/C Nanocomposites As Highly Selective Oil-Absorption Materials. *ACS Appl. Mater. Interfaces*, **2012**, *4* (5), pp 2420-2425.
- <sup>95</sup> Gui, X.; Zeng, Z.; Lin, Z.; Gan, Q.; Xiang, R.; Zhu, Y.; Cao, A.; Tang, Z. Magnetic and Highly Recyclable Macroporous Carbon Nanotubes for Spilled Oil Sorption and Separation. *ACS Appl. Mater. Interfaces*, **2013**, *5*, 5845-5850.
- <sup>96</sup> Calcagnile, P.; Fragouli, D.; Bayer, I.S.; Anyfantis, G.C.; Martiradonna, L.; Cozzoli, P.D.; Cingolani, R.; Athanassiou, A. Magnetically Driven Floating Foams for the Removal of Oil Contaminants from Water. *ACS Nano*, **2012**, *6*(6), 5413-5419.
- <sup>97</sup> <http://www.nanoparticles-microspheres.com/water-treatment-nanoparticles.html>
- <sup>98</sup> Chen, N.; Pan, Q. Versatile Fabrication of Ultralight Magnetic Foams and Application for Oil-Water Separation. *ACS Nano*, **2013**, *7*(8), 6875-6883.
- <sup>99</sup> Thanikaivelan, P.; Narayanan, N.T.; Pradhan, B.K.; Ajayan, P.M. Collagen based magnetic nanocomposites for oil removal applications. *Sci. Rep.* **2012**, *2*, 230.
- <sup>100</sup> Mohammadi, A.; Daemi, H.; Barikani, M. Fast removal of malachite green dye using novel superparamagnetic sodium alginate-coated Fe<sub>3</sub>O<sub>4</sub> nanoparticles. *Int. J. Biol. Macromol.*, **2014**, *69*, 447-455.

- <sup>101</sup> Yu, L.; Peng, X.; Li, Ji; Ni, F.; Luan, Z. Removal of As (V) and As(III) from water using Mn-doped maghemite nanoparticles. *Fresenius Environmental Bulletin*, **2014**, 23(2a), 508-515.
- <sup>102</sup> Zhang, X.; Chen, J.; Han, J.; Zhang, G. Preparation and evaluation of shell-core structured Fe<sub>3</sub>O<sub>4</sub>/MnO<sub>2</sub> magnetic adsorbent for Pb(II) removal from aqueous solutions. *Huanjing Kexue Xuebao*, **2013**, 33(10), 2730-2736.
- <sup>103</sup> Badruddoza, A. Z. M.; Shawon, Z. B. Z.; Tay, W. J. D.; Hidajat, K.; Uddin, M. S. Fe<sub>3</sub>O<sub>4</sub>/cyclodextrin polymer nanocomposites for selective heavy metals removal from industrial wastewater. *Carbohydrate Polymers*, **2013**, 91(1), 322-332.
- <sup>104</sup> Ha, D.-w.; Lee, Y.-J.; Kwon, J.-M.; Hong, H.-J.; Ko, R.-K.; Sohn, M.-H.; Baik, S.-K.; Kim, Y.-H. Preparation of magnetic Fe-Al binary oxide and its application in superconducting magnetic separation. *IEEE Transactions on Applied Superconductivity*, **2013**, 23(3, Pt. 2), 3700304/1-3700304/4.
- <sup>105</sup> Bakhshayesh, S.; Dehghani, H. Synthesis of magnetite-porphyrin nanocomposite and its application as a novel magnetic adsorbent for removing heavy cations. *Materials Research Bulletin*, **2013**, 48(7), 2614-2624.
- <sup>106</sup> Mahfouz, M. G.; Killa, H. M.; Sheta, M. E.; Moustafa, A. H.; Tolba, A. A. Synthesis, characterization, and application of polystyrene adsorbents containing tri-n-butylphosphate for solid-phase extraction of uranium(VI) from aqueous nitrate solutions. *J. Radioanal. Nucl. Chem.*, **2014**, 301(3), 739-749.
- <sup>107</sup> Wei, J.; Zhang, X.; Liu, Q.; Li, Z.; Liu, L.; Wang, J. Magnetic separation of uranium by CoFe<sub>2</sub>O<sub>4</sub> hollow spheres. *Chem. Engin. J.*, **2014**, 241, 228-234.
- <sup>108</sup> Zhou, C.; Zhang, Wenjie; W., Huixian; Li, H.; Zhou, J.; Wang, S.; Liu, J.; Luo, J.; Zou, B.; Zhou, J. Preparation of Fe<sub>3</sub>O<sub>4</sub>-Embedded Graphene Oxide for Removal of Methylene Blue. *Arabian Journal for Science and Engineering*, **2014**, 39(9), 6679-6685.
- <sup>109</sup> Hu, P.; Zhang, Y.; Tong, K.; Wei, F.; An, Q.; Wang, X.; Chu, P. K.; Lv, F. Removal of organic pollutants from red water by magnetic-activated coke. *Desalination and Water Treatment*, **2014**, Ahead of Print.
- <sup>110</sup> Deng, X.; Lin, K.; Chen, X.; Guo, Q.; Yao, P. Preparation of magnetic Fe<sub>3</sub>O<sub>4</sub>/Au composites for extraction of benzo[a]pyrene from aqueous solution. *Chemical Engineering Journal*, **2013**, 225, 656-663.
- <sup>111</sup> Zahoor, M. Magnetic adsorbent used in combination with ultrafiltration membrane for the removal of surfactants from water. *Desalination and Water Treatment*, **2014**, 52(16-18), 3104-3114.
- <sup>112</sup> Liu, H.; Lu, X.; Deng, C.; Yan, X. Highly sensitive MC-LR detection by matrix-assisted laser desorption/ionization time-of-flight mass spectrometry with magnetic mesoporous silica for fast extraction. *Rapid Communications in Mass Spectrometry*, **2013**, 27(21), 2515-2518.
- <sup>113</sup> Ma, X.; Wang, J.; Sun, M.; Wang, W.; Wu, Q.; Wang, C.; Wang, Z. Magnetic solid-phase extraction of neonicotinoid pesticides from pear and tomato samples using graphene grafted silica-coated Fe<sub>3</sub>O<sub>4</sub> as the magnetic adsorbent. *Analytical Methods*, **2013**, 5(11), 2809-2815.
- <sup>114</sup> Wang, Y.; Sun, Y.; Gao, Y.; Xu, B.; Wu, Q.; Zhang, H.; Song, D. Determination of five pyrethroids in tea drinks by dispersive solid phase extraction with polyaniline-coated magnetic particles. *Talanta*, **2014**, 119, 268-275.

- <sup>115</sup> Tian, M.-m.; Chen, D.-X.; Sun, Y.-L.; Yang, Y.-W.; Jia, Q. Pillararene-functionalized Fe<sub>3</sub>O<sub>4</sub> nanoparticles as magnetic solid-phase extraction adsorbent for pesticide residue analysis in beverage samples. *RSC Advances*, **2013**, 3(44), 22111-22119.
- <sup>116</sup> Eskandari, H.; Naderi-Darehshori, A. Preparation of magnetite/poly(styrene-divinylbenzene) nanoparticles for selective enrichment-determination of fenitrothion in environmental and biological samples. *Analytica Chimica Acta*, **2012**, 743, 137-144.
- <sup>117</sup> Beiraghi, A.; Pourghazi, K.; Amoli-Diva, M. Thiodiethanethiol Modified Silica Coated Magnetic Nanoparticles for Preconcentration and Determination of Ultratrace Amounts of Mercury, Lead, and Cadmium in Environmental and Food Samples. *Analytical Letters*, **2014**, 47(7), 1210-1223.
- <sup>118</sup> Cao, X.; Shen, L.; Ye, X.; Zhang, F.; Chen, J.; Mo, W. Ultrasound-assisted magnetic solid-phase extraction based ionic liquid-coated Fe<sub>3</sub>O<sub>4</sub>@graphene for the determination of nitrobenzenes in environmental water samples. *Analyst*, **2014**, 139(8), 1938-1944.
- <sup>119</sup> Ye, N.; Xie, Y.; Shi, P.; Gao, T.; Ma, J. Synthesis of magnetite/graphene oxide/chitosan composite and its application for protein adsorption. *Materials Science & Engineering, C: Materials for Biological Applications*, **2014**, 45, 8-14.
- <sup>120</sup> Liu, J.-W.; Yang, T.; Ma, L.-Y.; Chen, X.-W.; Wang, J.-H. Nickel nanoparticle decorated graphene for highly selective isolation of polyhistidine-tagged proteins. *Nanotechnology*, **2013**, 24(50), 505704/1-505704/8.
- <sup>121</sup> Bigdelifam, D.; Mirzaei, M.; Hashemi, M.; Amoli-Diva, M.; Rahmani, O.; Zohrabi, P.; Taherimaslak, Z.; Turkjolar, M. Sensitive spectrophotometric determination of fluoxetine from urine samples using charge transfer complex formation after solid phase extraction by magnetic multi-walled carbon nanotubes. *Analytical Methods*, **2014**, 6, 8633-8639.
- <sup>122</sup> Fazelirad, H.; Ranjbar, M.; Taher, M. A.; Sargazi, G. Preparation of magnetic multi-walled carbon nanotubes for an efficient adsorption and spectrophotometric determination of amoxicillin. *Journal of Industrial and Engineering Chemistry*, **2014**, Ahead of Print.
- <sup>123</sup> Beiraghi, A.; Pourghazi, K.; Amoli-Diva, M.; Razmara, A. Magnetic solid phase extraction of mefenamic acid from biological samples based on the formation of mixed hemimicelle aggregates on Fe<sub>3</sub>O<sub>4</sub> nanoparticles prior to its HPLC-UV detection. *Journal of Chromatography B: Analytical Technologies in the Biomedical and Life Sciences*, **2014**, 945-946, 46-52.
- <sup>124</sup> Heiligtag, F.J.; Airaghi Leccardi, M.J.I.; Erdem, D.; Süess, M.J.; Niederberger, M. Anisotropically structured magnetic aerogel monoliths. *Nanoscale*, **2014**, 6, 13213-13221.
- <sup>125</sup> Hua, R.; Li, Z. Sulfhydryl functionalized hydrogel with magnetism: Synthesis, characterization, and adsorption behavior study for heavy metal removal. *Chemical Engineering Journal*, **2014**, 249, 189-200.
- <sup>126</sup> Jiang, L.; Liu, P. Design of Magnetic Attapulgite/Fly Ash/Poly(acrylic acid) Ternary Nanocomposite Hydrogels and Performance Evaluation as Selective Adsorbent for Pb<sup>2+</sup> Ion. *ACS Sustainable Chemistry & Engineering*, **2014**, 2(7), 1785-1794.
- <sup>127</sup> Zhou, Y.; Fu, S.; Zhang, L.; Zhan, H.; Levit, M. V. Use of carboxylated cellulose nanofibrils-filled magnetic chitosan hydrogel beads as adsorbents for Pb(II). *Carbohydrate Polymers*, **2014**, 101, 75-82.
- <sup>128</sup> Yu, Z.; Zhang, X.; Huang, Y. Magnetic Chitosan-Iron(III) Hydrogel as a Fast and Reusable Adsorbent for Chromium(VI) Removal. *Industrial & Engineering Chemistry Research*, **2013**, 52(34), 11956-11966.

---

<sup>129</sup> Liu, Z.; Wang, H.; Liu, C.; Jiang, Y.; Yu, G.g; Mu, X.; Wang, X. Magnetic cellulose-chitosan hydrogels prepared from ionic liquids as reusable adsorbent for removal of heavy metal ions. *Chemical Communications*, **2012**, 48(59), 7350-7352.

<sup>130</sup> Lin, Y.-F.; Chen, J.-L. Magnetic mesoporous Fe/carbon aerogel structures with enhanced arsenic removal efficiency. *Journal of Colloid and Interface Science*, **2014**, 420, 74-79.

<sup>131</sup> Tang, S. C. N.; Yan, D. Y. S.; Lo, Irene M. C. Sustainable Wastewater Treatment Using Micro-sized Magnetic Hydrogel with Magnetic Separation Technology. *Industrial & Engineering Chemistry Research*, **2014**, 53, 15718–15724.

<sup>132</sup> Rosales-Landeros, C.; Barrera-Díaz, C.E.; Bilyeu, B.; Varela Guerrero, V.; Ureña Núñez, F. A Review on Cr(VI) Adsorption Using Inorganic Materials. *American Journal of Analytical Chemistry*, **2013**, 4, 8-16.

<sup>133</sup> Mahy, J. G.; Tasseroul, L.; Zubiaur, A.; Geens, J.; Brisbois, M.; Herlitschke, M.; Hermann, R.; Heinrichs, B.; Lambert, S. D. Highly dispersed iron xerogel catalysts for *p*-nitrophenol degradation by photo-Fenton effects. *Microporous and Mesoporous Materials*, **2014**, 197, 164-173.

